Geological Quarterly, 1999, 43 (4): 405–428

Facies and depositional environments of the Nida Gypsum deposits (Middle Miocene, Carpathian Foredeep, southern Poland)

Maciej BĄBEL

Bąbel M. (1999) — Facies and depositional environments of the Nida Gypsum deposits (Middle Miocene, Carpathian Foredeep, southern Poland). Geol. Quart., 43 (4): 405–428. Warszawa.

Seven facies (five primary and two diagenetic) and 12 subfacies are distinguished within the Nida Gypsum deposits which are a part of the widespread Middle Miocene (Badenian) evaporites of the Carpathian Foredeep cropping out in vicinity of Busko in southern Poland. Facies are defined as products of specific mechanisms of evaporitic deposition: syntaxial bottom growth of gypsum crystals, microbial gypsum deposition (mainly gypsification of organic mats), mechanical deposition and diagenetic and weathering processes. Primary facies and subfacies, and their uncommon sedimentary structures (such as: up to 3.5 m high bottom-grown gypsum crystals, several metres high selenitic domes, gypsum stromatolite domes, halite-solution collapse breccias) record a varied shallow water (0–5 m) evaporitic environment, controlled mainly by depth, salinity and climate.

Maciej Bąbel, Institute of Geology, Warsaw University, Żwirki i Wigury 93, PL-02-089 Warszawa, Poland; e-mail: babel@geo.uw.edu.pl
(received: June 9, 1999; accepted: September 20, 1999).

Key words: Carpathian Foredeep, Badenian, evaporites, facies analysis, selenites, alabasters, sedimentary structures, microbialites.

INTRODUCTION

The largest exposures the Paratethyan Middle Miocene evaporites in Poland occur in environs of Busko (Fig. 1). Evaporites of this area are known as the Nida Gypsum deposits (J. Flis, 1954; W. Bobrowski, 1963; S. Kwiatkowski, 1972, 1974; A. Wala, 1980). They are the best recognized part of the Miocene (Badenian) sulphate deposits of Carpathian Foredeep.

The author aims to reconstruct sedimentary history of the Nida Gypsum deposits after the facies analysis data. The following paper presents the descriptions and sedimentological interpretations of distinguished facies. The complete reconstruction of sedimentary history of the Nida Gypsum deposits is given in the separate paper (M. Bąbel, 1999*b*).

Hereafter the author introduces a somewhat different facies division of the Nida Gypsum deposits than the other authors (A. Kasprzyk, 1991, 1993*b*, *c*; T. M. Peryt *et al.*, 1994), as well as the present author himself (M. Bąbel, 1996). This division is based on the definition of the facies by E. Mutti and F. Ricci Lucchi (1975), adapted to studied evaporitic deposits. The chosen definition enhances depositional mechanisms as a base for facies distinguishing. Accordingly, the depositional mechanisms for each facies are characterized below without any stratigraphic and palaeogeographic context. However, spatial relations between facies and subfacies are used for environmental interpretations.

Term facies in this paper is defined as "...a layer or group of layers showing lithologic, geometric and sedimentologic characters which are different from those of adjacent beds..." (E. Mutti, F. Ricci Lucchi, 1975, p. 21). The facies "...is considered to be the product of a specific depositional mechanism or several related mechanisms..." (E. Mutti, F. Ricci Lucchi, 1975, p. 21). Some facies are also products of early diagenesis. The chosen facies definition is not purely descriptive but also interpretative because it involves the inferred depositional mechanism. The *depositional mechanism* is understand as the most significant mode (basic process or sedimentary event) in which the sediment is created at the basin

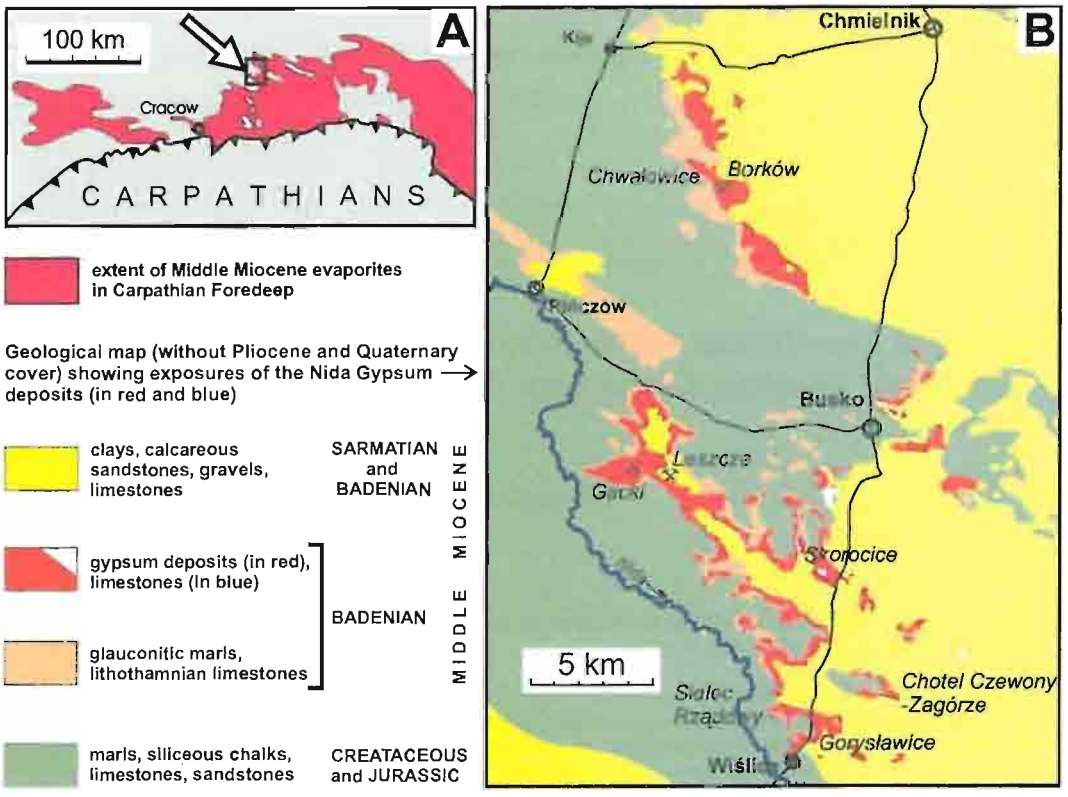

Fig. 1. Location of the Nida Gypsum deposits in southern Poland (A) and geologic map of the study area (B)

floor (or during early diagenesis). For the clarity of interpretation, in many places below, these fundamental mechanisms, processes or conditions of deposition, crucial for distinguishing of the facies, are considered separately and before the final environmental reconstructions. The recognized basic mechanisms of deposition together with related facies are listed in Table 1 and Fig. 2.

FACIES OF THE NIDA GYPSUM DEPOSITS

Basing on the main mechanisms of deposition seven facies are recognized in the Nida Gypsum deposits (which comprise gypsum, clay and carbonate sediments): the giant gypsum intergrowths, the gypsum crystal debris, the grass-like gypsum, the sabre gypsum, the microcrystalline gypsum, the porphyroblastic gypsum and the carbonate facies (Table 1, Fig. 2). The porphyroblastic and carbonate facies (Fig. 1), which are (with some exceptions) diagenetically modified and weakly recognized, are not discussed here. The five primary gypsum facies are subdivided into 12 subfacies. Traditional names introduced by earlier authors are adapted for designation of some facies (see references in Table 1). Illustrations and references to described facies and subfacies are listed in Table 1. Stratigraphy by A. Wala (1963, 1980), supplemented by M. Bąbel (1991), is used for location of illustrated outcrops and samples. Facies distribution is shown in M. Bąbel (1999*b*).

GIANT GYPSUM INTERGROWTHS

Description: This facies is composed of large crystals (several decimetres up to 3.5 m long), commonly arranged vertically and forming intergrowths similar to the $\bar{1}01$ twins. The facies do not exhibit layering except of rare dissolution surfaces. Two subfacies are distinguished according to crystal arrangement: the giant intergrowths with palisade and with non-palisade structure. Within the palisade intergrowths two subordinate subfacies showing a different crystal structure are recognized: the skeletal and the massive intergrowths. The rare clay subfacies of the giant intergrowths is built of isolated intergrowths and their aggregates (< 0.5 m in size) placed in black laminated clay. Spectacular load structures promoted by increased weight of growing crystals occur in the sediments below these aggregates.

Depositional mechanism: This facies was created almost exclusively by an upward bottom growth of gypsum crystals permanently covered with brine. The bottom brine was a salinity and a density range characteristic for gypsum precipitation (for marine brine a salinity between 150 and 320 g/l and a density from 1.12 to 1.21 g/cc[1]). The brine was nearly permanently saturated with calcium sulphates.

[1]If the brine composition was different than marine, and was similar to SO_4^{2-} rich waters of the Aral Lake, as suggested O. I. Petrichenko *et al.* (1997), the salinity and density for the start of gypsum and halite precipitation would be significantly lower. The gypsum begins to precipitate from the Aral water at a salinity of *ca.* 30 g/l and at a density 1.015 g/cc (I. N. Lepeshkov, N. V. Bodaleva, 1952).

Table 1

Facies of the Nida Gypsum deposits and references on their sedimentary environment

Facies	Depositional mechanisms	Subfacies	Illustrations	References	
				detailed	general
Carbonate facies	diagenetic processes			T. M. Peryt, A. Kasprzyk (1992*b*)	A. Gawel (1955), R. Nielubowicz (1961), S. Kwiatkowski (1972), B. Kubica (1992), J. Liszkowski (1992), A. Kasprzyk (1993*b*, *c*), J. Niemczyk (1995), T. M. Peryt *et al.* (1995), M. Bąbel (1996, 1999*b*), S. Hałas *et al.* (1995), T. M. Peryt (1996), O. I. Petrichenko *et al.* (1997), L. Rosell *et al.* (1998), A. Kasprzyk, F. Orti (1998)
Porphyroblastic gypsum	diagenetic processes			S. Kwiatkowski (1972, 1974), M. Bąbel (1996)	
Microcrystalline gypsum	mechanical deposition: settling of tiny crystals precipitated within brine, redeposition (which includes soft-sediment deformation, halite-solution subsidence and collapse)	breccias	Pl. X	S. Kwiatkowski (1970, 1972), M. Bąbel (1991, 1996), T. M. Peryt, A. Kasprzyk (1992*a*), T. M. Peryt, M. Jasionowski (1994)	
		alabasters			
		laminated gypsum	Pl. IX, X	S. Kwiatkowski (1972), T. Słomka (1979), J. Niemczyk (1985, 1988*a*), M. Bąbel (1991, 1999*a*)	
Sabre gypsum	syntaxial bottom growth of crystals (abundant creation of new crystals) and/or settling of crystals from brine column	wavy bedded	Pl. VIII, Fig. 1	J. Flis (1954), M. Bąbel (1986, 1996, 1998), O. I. Petryczenko *et al.* (1995)	
		flat bedded	Pl. VIII, Fig. 2		
Grass-like gypsum	alternated syntaxial bottom growth of crystals and microbial deposition (mainly gypsification of organic mats)	subfacies with stromatolitic domes	Pl. VII, Fig. 2	S. Kwiatkowski (1970, 1972), J. Golonka (1972), J. Niemczyk (1988*b*, *c*), A. Kasprzyk (1993*a*–*c*), M. Bąbel (1996), T. M. Peryt (1996), M. Bąbel *et al.* (1998)	
		subfacies with crystal rows	Pl. VII, Fig. 1		
		subfacies with alabaster beds	Pl. VI		
		subfacies with clay intercalations	Pl. IV, V		
Gypsum crystal debris	weathering and diagenetic processes		Pl. III, Fig. 2	J. Niemczyk (1988*c*), M. Bąbel (1996)	
Giant gypsum intergrowths	syntaxial bottom growth of crystals (rare creation of new crystals)	non-palisade intergrowths	Pl. III, Fig. 1	M. Bąbel (1984, 1996)	
		palisade intergrowths (skeletal and massive)	Pl. I Pl. III, Fig. 2 Pl. IV, Fig. 2	S. Kreutz (1925), A. Gawel (1955), B. C. Schreiber (1978), M. Bąbel (1984, 1987, 1990, 1996), T. M. Peryt (1996)	
		clay subfacies	Pl. II	M. Bąbel (1996)	

DEPOSITIONAL ENVIRONMENTS OF PALISADE SUBFACIES

The palisade subfacies crystallized on a basin floor, at a depth of no more than several metres, within the photic zone and beneath a relatively permanent pycnocline. Such a depth was necessary for constant existence of a stratified water body. Below the pycnocline, undestroyed by influxes of meteoric waters (J. K. Warren, 1982), the brine remained saturated with gypsum and its salinity was at the beginning of the Ca-sulphate precipitation phase (M. Bąbel, 1999*b*). The water above the pycnocline was unable to precipitate gypsum due to a lower salinity and hence this mineral crystallized exclusively within the bottom brine body. Organic compounds in brine (R. D. Cody, 1991) or a relatively low supersaturation with gypsum (R. A. Berner, 1980) significantly decreased the amount of new crystal seeds (*cf.* J. K. Warren, 1982). This allowed the intergrowths to grow *syntaxially* (M. I. Goldman, 1952) rarely being covered with crystal seeds. Long-termed syntaxial *competitive growth* (R. G. C. Bathurst, 1971) led to the palisade structure with extraordinary high component crystals. The crystal growth was interrupted only episodically by dissolution during larger salinity drops.

The growth of palisade crystals was dependent on a basin depth, oxygenation, presence of organic matter and clay influxes. The massive crystals grew within the better oxygenated shallower brines, on both coastal slopes and submerged isolated shoals (Fig. 3). The skeletal crystals originated within less oxygenated deeper brines, particularly in places where meteoric water loaded with clay flowed over the pycnocline. The skeletal forms crystallized in presence of some organic compounds which selectively adsorbed on specific gypsum faces framing intracrystalline pores (M. Bąbel, 1990). Presumably the adsorptive ability of these compounds was increased in the less oxygenated brine (see R. D. Cody, 1991).

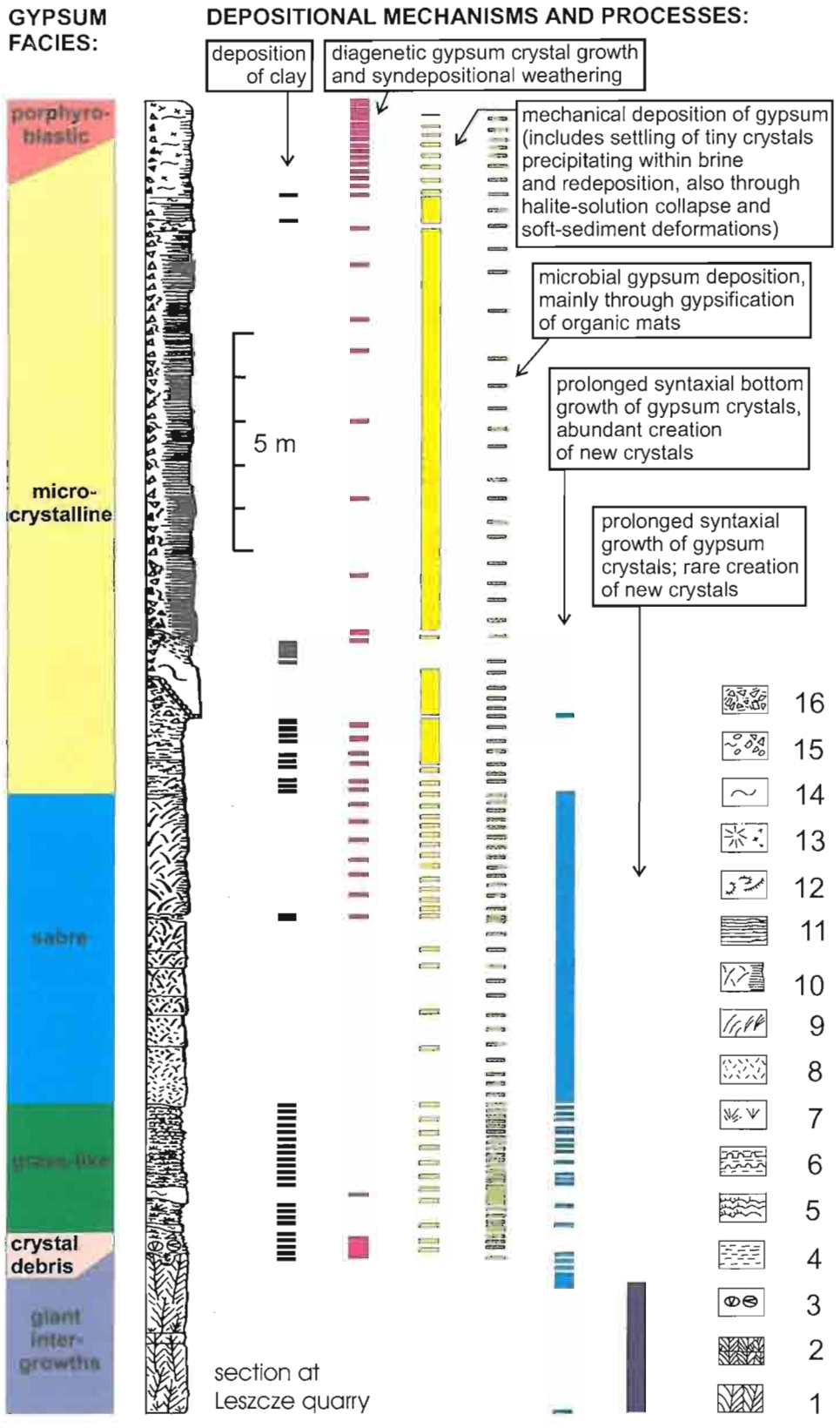

Fig. 2. Facies and depositional mechanisms of the Nida Gypsum deposits in typical section

1 — giant gypsum intergrowths, 2 — dissolution surface, 3 — debris of gypsum crystals, 4 — clay and clay-gypsum deposits, 5 — microbial gypsum domes (right) covered with bottom-grown gypsum crystals (left), 6 — microbial alabaster domes intercalated with clay, 7 — separate aggregates of bottom-grown gypsum crystals, 8 — rod-like bottom-grown gypsum crystals (< 15 cm), 9 — sabre gypsum crystals and their aggregates (> 15 cm), 10 — sabre gypsum crystals within laminated gypsum, 11 — flat and wavy laminated gypsum, 12 — arcuate and elliptical aggregates of gypsum crystals, 13 — radial aggregates of gypsum crystals (left) and gypsum porphyroblasts (right), 14 — compact fine-grained gypsum ("alabaster"), 15 — gypsum breccias with "alabaster" matrix, 16 — gypsum breccias with clay matrix

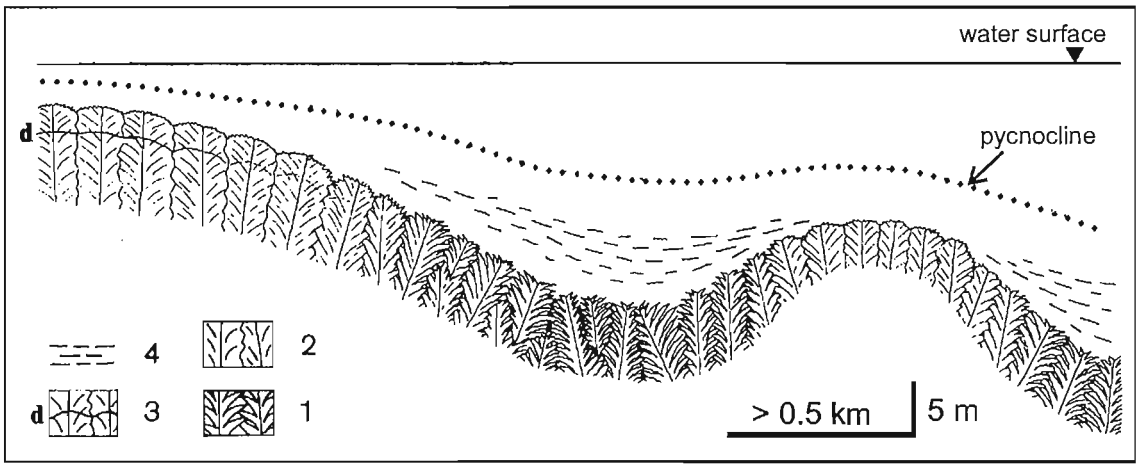

Fig. 3. Sedimentary environment of giant gypsum intergrowths with palisade structure

1 — skeletal crystals, 2 — massive crystals, 3 — dissolution surface (d), 4 — suspended clay matter

DEPOSITIONAL ENVIRONMENT OF CLAY SUBFACIES

The clay subfacies resulted from the growth of isolated gypsum crystals on a muddy substrate. The crystals grew simultaneously with fallout of clay particles from the water column. The isolated gypsum aggregates grew in a low oxygenated brine in the deepest basinal areas. In shallower and oxygenated brines the crystals grew as continuous crusts with a palisade structure. Similar rare facies are known from the Messinian evaporites (G. B. Vai, F. Ricci Lucchi, 1977).

DEPOSITIONAL ENVIRONMENT OF NON-PALISADE SUBFACIES

In this subfacies the syntaxial crystal growth was accompanied with frequent formation of new individuals growing on the surfaces of older crystals. Because of that the competitive growth was more complex and did not lead to the palisade structure. The crystals grew as aggregates, commonly horizontally and in a quasiradial manner. The depth was shallower than in the palisade facies and the intergrowths were less common. The crystal growth was probably highly disturbed by fluctuation of the pycnocline and salinity, or episodic emersions. Some parts of that subfacies represents regenerated crystals of weathered crystalline debris formed during long-termed emersion (see below).

GYPSUM CRYSTAL DEBRIS

Description: Bed of a crystal debris (up to 0.5 m thick) covers locally the apices of the giant intergrowths. It is overlain by the grass-like gypsum subfacies with clay intercalations. The debris is a mixture of clay and broken, abraded and dissolved crystals, up to 0.5 m long. It also contains small, rounded pieces of gypsified organic mats. The debris fills 10–30 cm deep depressions between apices of intergrowths which are flatted due to dissolution. The deeper depressions contain up to several centimetres large aggregates of lenticular crystals grown *in situ* within clay.

Interpretation: The debris is a product of emersion of the giant intergrowths apices and later specific weathering and diagenetic processes acting in a coastal sabkha-like flat, periodically overflooded with meteoric waters loaded with clay (Fig. 4). Similar crystalline debris occur in recent emerged salinas (F. Ortí Cabo *et al.*, 1984, figs. 12.3, 16.4; B. W. Logan, 1987).

GRASS-LIKE GYPSUM

Description: This facies is characterized by thin layering (0.1–20 cm) and the *grass-like structures* (*sensu* G. Richter-Bernburg, 1973, fig. 7b) formed by a single generation of bottom-grown gypsum crystals. They create 0.1–20 cm thick crusts, or rows, intercalated with laminae or layers of fine-grained gypsum and/or clay. Larger grass-like crystals are straight and similar in morphology and growth pattern to the giant intergrowths (Fig. 5A).

The grass-like facies encloses four subfacies: (I) with crystal rows, (II) with stromatolitic domes, (III) with clay intercalations, and (IV) with alabaster beds.

Depositional mechanisms : Excluding subordinate processes (current and wave redeposition, slumping, suspension fallout of clay, diagenetic gypsum crystallization), the grass-like facies was deposited by two alternately acting mechanisms: (I) syntaxial bottom-growth of large crystals (B. C. Schreiber *et al.*, 1976), and (II) microbial gypsum deposition (*microbial sensu* R. V. Burne, L. S. Moore, 1987; i.e. with the origin influenced by microbes; R. V. Burne, L. S. Moore, 1993).

The former mechanism was the same as in the case of giant intergrowths and required a permanent, or only shortly interrupted, period of a high salinity of bottom brines staying saturated with gypsum (B. C. Schreiber *et al.*, 1976; J. K. Warren, 1982; F. Ortí Cabo *et al.*, 1984). The syntaxial growth

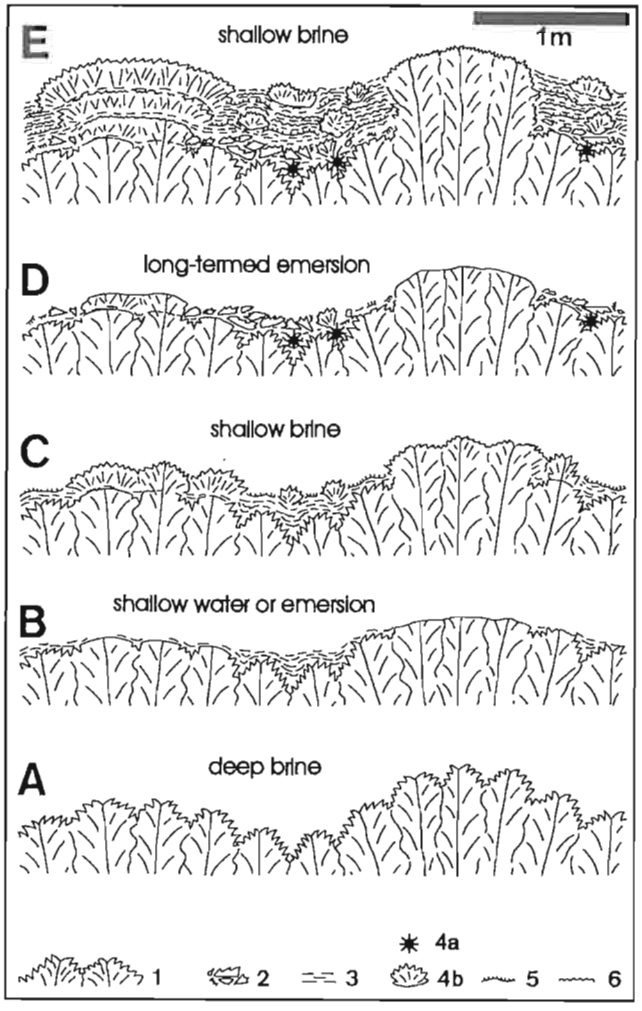

Fig. 4. Deposition of gypsum crystal debris facies and grass-like gypsum subfacies with clay intercalations during shallowing and emersion of giant gypsum intergrowths: **A** — palisade growth of giant intergrowths in a deep brine, **B** — shallowing and influx of meteoric waters with clay; dissolution of highest crystal apices and clay deposition in depressions, **C** — deposition in shallow brine; growth of grass-like crystals, syntaxial growth of intergrowths, gypsification of organic mats, **D** — long-termed emersion: destruction and weathering of gypsum crystals; diagenetic growth of lenticular gypsum aggregates in clay-filled depressions, **E** — deposition in shallow brine; accretion of domal selenitic structures built of grass-like crystals (left) and of giant intergrowths (right), and simultaneous deposition of clay and microbial gypsum in depressions

1 — giant gypsum intergrowths; 2 — broken, corroded and abraded gypsum crystals; 3 — clay; 4a — aggregates of lenticular gypsum crystals; 4b — separate aggregates of grass-like gypsum crystals; 5 — wavy laminated organic mats encrusted with small gypsum crystals; 6 — gypsified organic mats with knobby morphology

in the shallow brine (as in the case of studied facies) appear to be controlled mainly by a relatively high level of supersaturation with calcium sulphates accelerating the rate of gypsum growth (J. Kushnir, 1981; J. K. Warren, 1982). Hence the grass-like crystals commonly represent periods of prolonged intensive evaporation. Their growth requires lack of any substantial influxes of less saline waters (J. K. Warren, 1982) and in recent marine salinas is common within a salinity range 200–300 g/l (F. Ortí Cabo *et al.*, 1984; D. Geisler-Cussey, 1997).

The microbial deposition is assumed to be responsible for sedimentation of fine-grained gypsum with common relics or traces of organic mats (Pl. VI, Fig. 1). The bulk of similar fine-grained gypsum in the recent salinas is apparently connected with the presence of organic mats (J. Kushnir, 1981; F. Ortí Cabo *et al.*, 1984) strongly suggesting microbially related origin of sulphates. Such mats in salinas evidently create a substrate or locus for the precipitation or deposition of fine gypsum grains, exactly as it is required by the definition of microbialite (R. V. Burne, L. S. Moore, 1987). These grains are not any products of microbes, or their metabolic activity, but result from exclusively chemical precipitation in specific environment created by benthic microbial communities. Such precipitation is commonly promoted by Ca-sulphate concentration rise due to evaporation, but also by mixing of brines of different salinities (host brines with the brines inflowing from other areas; F. Ortí Cabo *et al.*, 1984; M. Bąbel, 1999*a, b*). Biochemical precipitation of gypsum was documented only for a few micro-organisms and is highly controversial. The other common mode of microbial deposition, trapping and binding of detritus by cohesive cyanobacterial mats (R. V. Burne, L. S. Moore, 1987), was recognized only in one of the studied subfacies (subfacies with stromatolitic domes).

The microbial gypsum deposition is commonly accomplished through *gypsification* of organic mats (J. M. Rouchy, C. L. V. Monty, 1981; F. Ortí Cabo *et al.*, 1984; A. Kasprzyk, 1993*a*) which lead to perfect preservation of mat morphology (as in the studied facies). The gypsified mats are deposited in marine salinas in the first phase of gypsum precipitation (a salinity from 150 to 230 g/l), and occupy the area of occurrence of the laminated cyanobacterial mats (F. Ortí Cabo *et al.*, 1984). It seems that the best conditions for gypsification of organic mats exist during oscillations of salinity at the beginning of gypsum precipitation phase (a salinity 150 g/l for marine brine), and associated significant drops in Ca-sulphate concentration (*cf.* J. M. Rouchy, C. L. V. Monty, 1981). Salinity drops within the gypsum precipitating brine of a higher salinity (200–300 g/l) do not produce gypsified mats (D. Geisler-Cussey, 1997). Refreshments and salinity falls below 150 g/l stop the gypsum deposition and enable the bloom of micro-organisms, mainly cyanobacteria, which create thick mats. Evaporative salinity increase causes renewal of the gypsum precipitation and limits accretion of the mats. They commonly disappear at the beginning of gypsum precipitation phase. Some authors believe that it is because cyanobacteria living in the mats are incapable of growing at salinities over 150 g/l (A. Cornée *et al.*, 1992). However, many cyanobacteria tolerate higher salinities, commonly up to *ca.* 230 g/l (G. M. Friedman, W. E. Krumbein, 1985; D. Giani *et al.*, 1989). The disapperance of the mat is related to its smothering and covering by precipitating gypsum (R. J. Hite, D. E. Anders, 1991). The gypsum crystal seeds nucleate on the substrate; both on the mat surface (A. J. Fersman, 1919; W. E. Krumbein, Y. Cohen, 1977; B. C. Schreiber, 1978) and within the mat (F. Ortí Cabo *et al.*, 1984; M. A. M. Aref,

1998). Encrustation of the mat surface with gypsum preserves details of its morphology producing the gypsified mat. Crystallization within the mat, common in emerged sabkhas (H. Dronkert, 1977; H. E. Reineck *et al.*, 1990), displaces a soft organic tissue and destroys its structure leading to non-laminated, frequently nodular gypsum sediments (W. E. Krumbein, Y. Cohen, 1977; J. Kushnir, 1981; F. Ortí Cabo *et al.*, 1984). Repeated growth of the mat and its gypsum encrustation produce gypsified organic mat deposits representing typical gypsum microbialites. The conditions favourable for gypsification may occur on evaporitic shoals periodically flooded with less saline, either marine or meteoric waters. In the studied facies clastic clays suggest large input of meteoric waters.

Summarizing, a salinity was a main factor controlling the deposition of grass-like facies; the upright crystals grew within the brine saturated with calcium sulphates nearly permanently; the bulk of fine-grained gypsum was deposited during oscillations of a salinity at the beginning of gypsum precipitation phase.

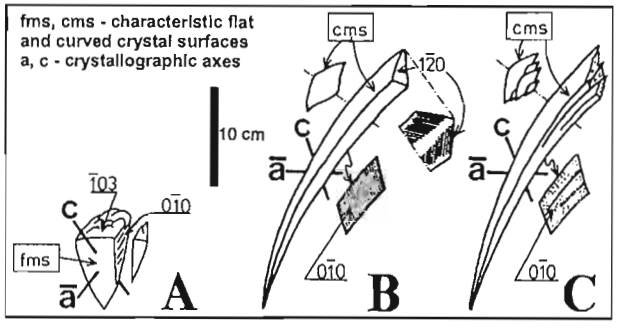

Fig. 5. Bottom-grown gypsum crystals typical of the grass-like facies (A) and sabre facies (B and C); note different arrangement of inclusions on 010 cleaved surfaces

SUBFACIES WITH CLAY INTERCALATIONS

Description: This is the most variable subfacies. It is composed of aggregates or separate rows of large (several to *ca.* 30 cm) grass-like crystals, scattered or intercalated within thin-layered clay-carbonate-gypsum deposits containing frequent thin (< 0.5 cm) crusts of bottom-grown crystals and gypsified organic mats.

The large crystals form domal structures of variable morphology surrounded by clay-carbonate-gypsum deposits. The domes consisted of upright crystals include both isolated mounds and platformal structures a dozen or so metres across. The mounds are commonly coated with alternating layers of microbial gypsum and bottom-grown crystals and grade upward into larger metric sizes domal structures. Small alabaster mounds with massive cores and brain-like top surfaces are also present. The clay-carbonate-gypsum deposits, commonly found in large depressions between the described domes, form thin (< 2 cm) alternating sequences composed of (from the base to the top): (I) clay lamina, (II) calcium carbonate lamina, (III) fine-grained gypsum lamina, or laminae, usually with knobby top surface representing morphology of an organic mat, (IV) continuous crust or patches of bottom-grown gypsum crystals covering the highest knobs of underlying laminae. The (II) and (IV) interval is frequently absent. Some clay-gypsum deposits occur in shallow (< 15 cm) and broad (up to several metres) channel structures. Channels, commonly with large bottom-grown crystals on their banks, are filled with mixed gypsum and clay material, intraclasts of gypsified mats and broken crystals.

Interpretation: The subfacies represents a coastal evaporitic shoal or flat seasonally overflooded with clay loaded meteoric waters transported by sheet floods (B. W. Logan, 1987; A. V. Arakel, 1980). As in many recent salinas, the gypsum deposition was controlled by topography (N. Dulau, N. Trauth, 1982; J. M. Rouchy, 1982; F. Ortí Cabo *et al.*, 1984). The grass-like crystals grew preferentialy on elevated shallow areas (Fig. 4C, E). The brines there reached the highest temperature and thus evaporated more intensively, attaining a higher salinity than in depressions. This enabled the more quick and ubiquitous growth of gypsum crystals which created clusters and domes. Similarly as in salinas the domes growing on the highest elevations were grouped side by side, there attaining the largest sizes and frequency (J. M. Rouchy, 1982; F. Ortí Cabo *et al.*, 1984). Small isolated alabaster mounds grew as in some recent seasonally drying salinas covered with thick organic mats (H. Dronkert, 1977).

Clay deposition was likewise controlled by topography. Sheet floods transported mud predominantly along more or less broad depressions of the flat and covered them with a clay. This clay significantly has limited the gypsum crystallization (Fig. 4C, E). Lack of clay cover on elevations enabled the gypsum crystals easy syntaxial growth. The clay-carbonate-gypsum sequences reflect salinity fluctuations promoted by such influxes of meteoric waters. Sheet floods concentrated into streams erroded channels infilled subsequently with detrital deposits derived from destruction and reworking of the substrate.

SUBFACIES WITH ALABASTER BEDS

Description: The subfacies is built of up to 0.5 m thick alabaster beds, intercalated with thin crusts of grass-like crystals. Alabaster reveals crenulated lamination formed by gypsification of hummocky surfaces of organic mats. Homogeneous or slightly nodular alabasters represent gypsified unlaminated mats or laminated mats destroyed by displacive fine gypsum crystals.

Interpretation: The alabaster was deposited by an intensive precipitation of abundant tiny gypsum crystals on the basin floor in areas sheltered from currents, waves and clay supply. At least partly it is a microbialite formed by gypsification of organic mats. Snow-white colour of many alabasters suggests, however, a low content of organic matter and lack of organic mats. Such a white alabaster was probably deposited by an intensive chemical precipitation from a highly concentrated *brine sheet* less than a few centimetres thick (B. W. Logan, 1987; T. M. Peryt, 1996). Due to a minimal depth and isolation from meteoric water floods, brine was very hot

and highly saline nearly permanently. During evaporation it could attain a very high supersaturation with Ca-sulphate, allowing continuous and spontaneous nucleation of gypsum. Abundant gypsum precipitation in a semi-emerged, highly saline environment, likely close to a halite saturation at the level of 300 g/l, smothered and suppressed organic mats (*cf.* A. Cornée *et al.*, 1992). Emerged mats were destroyed by diagenetic growth of gypsum crystals in a sabkha environment (A. Kasprzyk, 1993*b*).

SUBFACIES WITH CRYSTAL ROWS

Description: Up to 0.3 m thick rows of upright crystals are intercalated with thin layers of microbial fine-grained gypsum. The grass-like crystals frequently show large intercrystalline fenestral pores roofed with fine-grained gypsum.

Interpretation: Growth of thick rows of grass-like crystals required a relatively permanent supersaturation of brine with gypsum. Such conditions are typical of density stratified saline pans. Gypsified organic mats indicate shallow brines, a drop of a salinity and its oscillations around a level of gypsum saturation. Fenestral intercrystalline pores were formed by gypsification of thick organic mats covering the separate apices of grass-like crystals (M. Bąbel, 1996). Massive rows of crystals grew on elevations and their slopes similarly as massive palisade intergrowths.

SUBFACIES WITH STROMATOLITIC DOMES

Description: The flat-topped, up to 32 cm high gypsum domes in that subfacies were described as algal stromatolites by S. Kwiatkowski (1970, 1972). They are built of alternated crusts of bottom-grown crystals, gypsified knobby organic mats and laminae of "clastic" sugar-like gypsum with both reverse and normal grading. The clastic laminae commonly lie on uneven knobby substrate and show smooth top surfaces. Locally they create flat lenticular bodies resembling channel infillings. Fenestral pores occur near bottom-grown crystals.

Interpretation: The domes show complex, both chemical and microbial origin. Small grass-like crystals and gypsified organic mats were formed in a relatively calm environment during salinity oscillations at the beginning of gypsum precipitation phase. The sugar-like gypsum was at least partly deposited mechanically during increased wave action. The mechanical deposition is suggested by features of the infilling and flatten of a substrate relief by these grainy laminae (M. Bąbel, 1996, fig. 12; *cf.* L. A. Hardie, H. P. Eugster, 1971). On the other hand such laminae run concordantly with dome shapes suggesting that gypsum grains were trapped and bound on domes slopes by cohesive organic mats (B. C. Schreiber *et al.*, 1982), exactly as in a concept by S. Kwiatkowski (1970, 1972) who applied the definition of algal stromatolites after B. W. Logan *et al.* (1964) for these structures. Since such trapping and binding is diagnostic for stromatolites *sensu* B. W. Logan *et al.* (1964) and S. M. Awramik and L. Margulis (1974 in M. R. Walter, 1976), and for microbialites (R. V. Burne, L. S. Moore, 1987), both the name of stromatolite and microbialite fit to the described structures.

GENERAL ENVIRONMENTAL INTERPRETATION OF THE GRASS-LIKE FACIES

The discussed subfacies in the lower part of the Nida Gypsum deposits show the following arrangement (M. Bąbel, 1999*b*, fig. 2). The subfacies with crystal rows and stromatolitic domes are present mainly on the north, whereas the subfacies with clay intercalations and alabaster beds nearly exclusively on the south of the studied area. The rarest subfacies with alabaster beds occurs only in three outcrops directly overlying the giant intergrowths and passing laterally into subfacies with clay intercalations. The subfacies with stromatolitic domes occur only in layer **e** intercalating the subfacies with crystal rows and passing laterally to the south into subfacies with clay intercalations particularly rich in clay laminae (layer **e** in the Wiślica area; M. Bąbel, 1999*b*).

Such spatial relations allow to reconstruct the environment of large evaporitic shoal or flat shallowing to the south, toward the land area being the source of clastic clay (Fig. 6). A salinity on this shoal oscillated at the beginning of gypsum precipitation phase. Salinity drops corresponded with inflows of meteoric waters. Shoal topography and a distance from the coastline have controlled the distribution of grass-like subfacies. The subfacies with clay intercalations was deposited close to the coastal mudflats inflooded by meteoric rain waters. The alabaster beds subfacies was deposited on elevations unaffected by muddy sheet floods. The subfacies with crystal rows represents pan-like depressions localized far away from the coast and isolated from a clay supply. The stromatolitic domes subfacies was deposited on windward, affected by waves and wave currents slopes of the deeper brine-filled pans. Deposition of this subfacies coincided with numerous muddy sheet floods, related to increased frequency of rains, in the southern coastal area. Presumably frequent refreshments promoted microbial blooms and contributed to accretion of stromatolitic domes.

The elongation of stromatolite domes (S. Kwiatkowski, 1970) and coincident inclination of grass-like crystals in adjacent layers **d** and **f** (Fig. 2; M. Bąbel, 1996) suggest a current direction that moved from the north to the south of the study area. This direction is in accordance with the general brine flow pattern in the foreland basin, i.e. with the longshore counterclockwise brine movement along the northern coast of the basin (M. Bąbel, 1998; A. Roman, 1999). The southern clay-gypsum coastal flat was thus periodically flooded both with the brine (mainly from the north, but also from the east), and, at times, with meteoric waters — from the south (Fig. 6). Morphology of the mats from this coastal area was very variable due to these changing salinity conditions. The brine influxes led to a rapid gypsification of organic mats (Fig. 4C, E) and to perfect and spectacular preservation of their microbial structures.

SABRE GYPSUM

Description: This facies is characterized by curved ("sabre") crystals (15–95 cm long; Fig. 5B, C) and thick bedding (0.2–1.5 m). The crystals grew upward and simultaneously curved laterally due to crystal lattice twisting. The long cry-

stals are covered with subsequent generation of smaller crystals and the 100 twins. The crystals commonly show concordantly oriented apices which all, or nearly all, are turned horizontally in the same direction. This orientation was caused by a constant and long-lasting brine current flowing over the crystal apices during their growth on the basin floor (H. Dronkert, 1985; M. Bąbel, 1996). Locally the giant several metres high and up to 13 m wide domal structures occur within the sabre gypsum. They are primary forms (J. Tokarski in J. Flis, 1954; M. Bąbel, 1986) similar to the recent gypsum domes, up to 2 m high, growing at a depth of several metres in salinas of Australia (J. K. Warren, 1982).

The sabre gypsum encloses: (I) flat bedded subfacies, entirely built of bottom-grown crystals, and (II) wavy bedded subfacies, with bottom-grown crystals scattered within laminated fine-grained gypsum. The flat bedded subfacies is composed of large crystals stacked one on the other. The bedding is created by thin intercalations of fine-grained gypsum or, rarely, by dissolution surfaces. The bottom-grown crystals form massive or porous structure. The pores are empty or filled with fine-grained gypsum, in places with calcite and dolomite. The skeletal gypsum *sensu* M. Bąbel (1981) and A. Kasprzyk (1993*b*), built of small (< 15 cm) sabre crystals, is included into this subfacies.

The wavy bedded subfacies demonstrates uneven layering and soft-sediment deformations. The last ones include load structures beneath the sabre commonly aggregated crystals which grew on a soft uncemented gypsum substrate similarly as *selenitic nucleation cones* described by H. Dronkert (1985). Folds related to sediment creep and slump are common. Sparse debris flows contain redeposited sabre crystals. The crystals are commonly broken due to compaction. Fine-grained gypsum deposits create small domal structures locally with calcitized algal filaments.

Depositional mechanisms: The flat bedded subfacies was created by syntaxial bottom growth of crystals associated with frequent formation of new individuals and the 100 twins. The new crystals accreted on surfaces of older ones, especially on their upper faces. Episodic refreshments led to development of microbial fine-grained gypsum and dissolution surfaces. Occasional currents eroded the substrate and redeposited gypsum sands.

Depositional mechanisms in the wavy bedded subfacies were complex. Bottom growth of large crystals was accompanied with settling of tiny crystals from a brine column and microbial deposition of fine-grained gypsum. The fine-grained gypsum underwent an early cementation which obliterated its lamination. Cementation commonly has occurred within and around the nucleation cones (Pl. VIII, Fig. 1). The remaining uncemented fine-grained gypsum was soft and subjected to deformations which included those generated by gravity mass movements.

DEPOSITIONAL ENVIRONMENTS OF SABRE GYPSUM FACIES

The flat bedded subfacies was deposited in more than 1 m deep brine. Such a depth was necessary for existence of a permanent density stratification maintaining bottom growth of large crystals and giant domes. This growth was disturbed

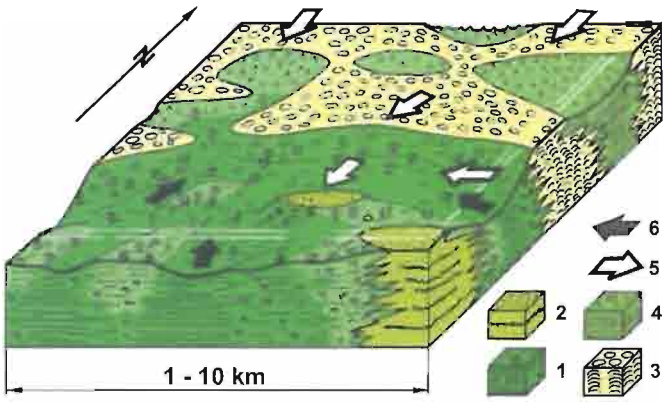

Fig. 6. Evaporitic shoal representing depositional area of the grass-like gypsum of lithosome **B**; relief exaggerated; northern part correspond to the Pińczów area, the southern one represents the Wiślica area (see M. Bąbel, 1999*b*, fig. 1B)

1–4 — subfacies of grass-like gypsum: 1 — with clay intercalations, 2 — with alabaster beds, 3 — with stromatolitic domes, 4 — with crystal rows; 5 — brine currents; 6 — sheet floods of meteoric waters loaded with clay

by refreshments, recorded by dissolution surfaces, and microbial gypsum deposition which indicate a relatively shallow depth (J. K. Warren, 1982; F. Ortí Cabo *et al.*, 1984). A porous and a massive structure, and local presence of microbial gypsum, similarly as in the case of giant intergrowths, reflect variations in depth and oxygenation of brines. The brine was more saline than in the giant intergrowths environment (M. Bąbel 1996; L. Rosell *et al.*, 1998).

The sabre crystals have their crystallographic equivalents in many marine salinas (< 1 m deep) although the crystals from salinas are only a few milimetres in size, and rarely more than 10 cm (A. E. Fersman, 1919; B. C. Schreiber *et al.*, 1977; F. Ortí Cabo *et al.*, 1984; D. Geisler-Cussey, 1986). Only in some deep (several metres) salinas of Australia do gypsum crystals show comparatively large sizes (J. K. Warren, 1982).

The giant domes accreted on the elevated areas of evaporitic shoal during its drowning and possible rise of a salinity (Fig. 7; M. Bąbel, 1999*b*). The domes occur there locally and commonly with the grass-like gypsum subfacies with alabaster beds directly below. This subfacies represents former shoal elevations (Fig. 6). Such elevations were commonly overgrown with the small gypsum domes built of separate aggregates or rows of grass-like crystals (Fig. 7A). During the drowning of the shoal the small domes developed into larger forms due to syntaxial growth of crystals below a pycnocline, in a more saline, deeper brine. The domes were covered with successive layers of sabre gypsum which accreted concordantly with the initial bottom convexities. The giant domes occur in clusters, one near the other, passing laterally into a flat or wavy bedded sabre gypsum deposited in nearby depressions (Fig. 7B). In places the giant domes accreted over the domes present within the grass-like subfacies with clay intercalations (Fig. 4E).

The wavy bedded subfacies was deposited in density stratified brines. The bottom crystallization of gypsum and its early cementation was strongly inhibited, as indicated by

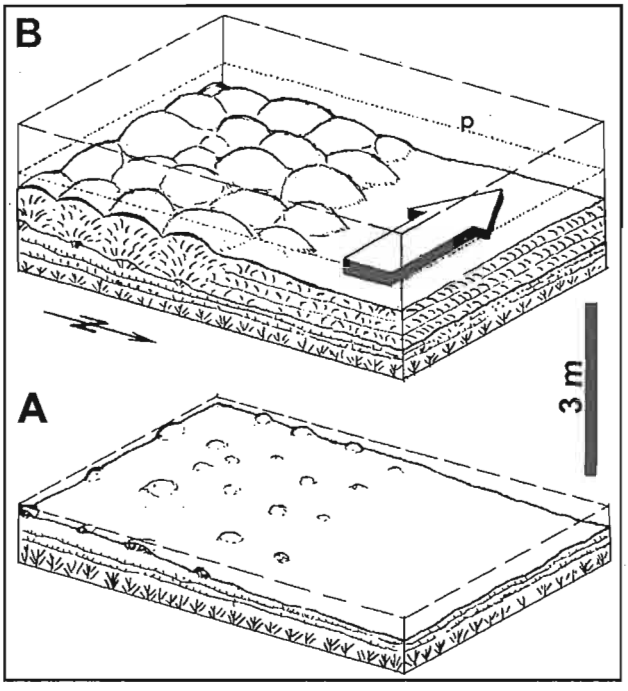

Fig. 7. Development of giant sabre gypsum domes during drowning of elevated area of evaporitic shoal at Skorocice: **A** — deposition of grass-like gypsum (subfacies with alabaster beds) on a slope of evaporitic shoal (see Fig. 6), **B** — sabre gypsum deposition and accretion of giant domes

p — pycnocline; arrow indicates brine current; note that giant domes were accreted on the small domal structures scattered on the shoal elevation

associated soft-sediment deformation. Tiny gypsum crystals precipitated within the brine column, although they could also derive from redeposition. Algal remnants suggest a shallow photic zone. The sedimentary environment was transitional to described below for the microcrystalline facies (M. Bąbel, 1999*b*). In this peculiar environment the gypsum crystallization at the bottom was inhibited by lowered concentration of Ca^{2+} and/or SO_4^{2-} within the highly saline brine below a pycnocline (M. Bąbel, 1999*a*).

MICROCRYSTALLINE GYPSUM

Description: This facies includes many lithologic varieties (subfacies) which are built of macroscopically invisible crystals (< 300 μm in size). The most widespread subfacies are laminated gypsum, alabasters or compact gypsum, and breccias. The facies locally contains thick clay intercalations.

Depositional mechanisms: They include processes characteristic for the *mechanical* deposition *sensu* Sander (B. Sander, 1970; R. G. C. Bathurst, 1971), but also the microbial deposition and diagenesis.

LAMINATED GYPSUM

Description: The subfacies is built of thin (< 1 mm) flat laminae. They are usually visible only due to colour differences between clear gypsum and gypsum with rod-like algal remnants or ghosts and finely disseminated organic-clay matter. Algal remnants are mostly crushed. Intercalated clay laminae locally contain floral detritus. Rare coarser-grained laminae (<1 cm thick) show normal grading and, exceptionally, low-angle cross-lamination. Wash-out surfaces commonly locate along lamination and are hardly visible (Pl. IX, Fig. 1). Frequent traces of single halite cuboids (< 2 cm) lay with their larger faces parallel to lamination. Very common soft-sediment deformations include complex folds, commonly slump ones, microfaults, load, flow, and fluidization structures. Microbial domal structures occur in places (M. Bąbel, 1996, fig. 24). They were formed by local regrowth and cementation of tiny crystals settling from a brine column in a very calm environment (M. Bąbel, 1996). The "rigid" clasts of such domes are found within cohesive flows and slumps. Rare small aggregates of gypsum crystals grew on the basin floor as loose nodules not cemented to the substrate. They occur both as clasts within gravity flow deposits and as a lag on some wash-out surfaces.

Depositional mechanisms and environment: Laminated gypsum is a product of periodic or episodic settling of tiny crystals from a brine column. They derived from both redeposition and direct precipitation within the brine. The redeposition is evidenced by wash-out structures, low angle cross-lamination, gravity flow and slump deposits. The laminae were deposited from basin-wide suspension clouds (triggered by storm waves), or from low density turbidity currents (generated by slumps, gravity flows, strong currents). The laminae built of crystals which precipitated within the brine and settled on the bottom (without redeposition) are recognizable under a scanning microscope (M. Bąbel, 1996, fig. 23). The crystals are euhedral and stacked one on the other with their larger faces parallel to the lamination (resembling the *pile of bricks* or *cumulative* structures; T. Lowenstein, 1982). In this subfacies gypsum generally did not precipitate at a sediment-brine interface. However, halite crystals grew from a highly saline brine on the basin floor. Deformation is commonly related to early diagenetic dissolution of halite within soft gypsum deposits.

ALABASTERS OR COMPACT GYPSUM

Description: These deposits are extremely differentiated. They appear to be derived from primary laminated gypsum as indicated by relics of disturbed lamination visible in many alabasters as well as gradational transitions from laminated gypsum into alabasters. The alabasters show also continuous transitions both into the breccias and the diagenetic porphyroblastic gypsum facies. Most alabasters reveal flow structures often caused by salt solution of thin beds soon after burial.

Abundant solution-subsidence deformation structures are commonly brachyfolds without any constant vergence.

Mechanisms and environment of deposition: Many alabasters represent solution residua after synsedimentary or early diagenetic dissolution of halite intercalated within primary gypsum laminae (M. Bąbel, 1991). The synsedimentary residua record a specific environment of the sulphate-chloride deposition. They were deposited during salinity changes of bottom brines at the beginning of halite precipitation phase (for marine brine a salinity *ca.* 300 g/l). Frequent salinity oscillations led to multiple crystallization and dissolution of halite on the basin floor. The floor was simultaneously periodically or episodically covered with tiny gypsum crystals settling from the brine column. Diagenetic crystallization and regrowth of these tiny crystals additionally obliterated lamination within the solution residuum. The other alabasters are products of redeposition (by gravity flows, and mainly cohesive flows), fluidization, microbial deposition, dehydration and rehydration (S. Kwiatkowski, 1972; A. Kasprzyk, 1995).

BRECCIAS

Many varieties of breccias occur in the discussed facies. Most of them grade into alabasters and are halite solution-collapse breccias. The latter locally enclose the whole upper part of the section and occur in solution-collapse chimneys. Some breccias are gravity flow deposits.

DEPOSITIONAL ENVIRONMENT OF MICROCRYSTALLINE FACIES

Flat parallel lamination and extremely small grains suggest a very calm environment where strong bottom currents and gravity mass movements were only short-termed events. Nearly complete lack of bottom-grown crystals and very common soft-sediment deformation prove that gypsum crystallized neither within a sediment nor at a sediment-brine interface. The gypsum grains remained loose or only slightly consolidated and generally did not undergo an early cementation. Although gypsum crystallization both on a bottom and within sediments was strongly inhibited, this mineral precipitated within the upper part of brine column. Contrary to gypsum, halite crystallized directly at the bottom. The described features are the result of the complex structure and composition of density stratified brines (M. Bąbel, 1996). The stagnating bottom brines were probably highly anoxic and hence significantly stripped of sulphate ions necessary for gypsum crystallization. These brines developed at the beginning of halite precipitation phase (reaching a salinity of *ca.* 300 g/l and a density of 1.21 g/cc; data for marine brines) which means that they were also strongly impoverished in Ca^{2+} equally needed for gypsum crystal growth (M. Bąbel, 1999*b* with references therein). The gypsum precipitated within the upper brine layer not only due to evaporation but also due to mixing with the Ca^{2+} and SO_4^{2-} rich oxygenated brines inflowing from other parts of evaporite basin (see M. Bąbel, 1999*a*, *b* for details). Bottom brine salinity oscillations, either because of influx of meteoric waters or of less saline brines from outlying areas, led to multiple crystallization and dissolution of halite and to deposition of residual alabasters. Such dissolution was facilitated by the shallow (commonly < 1 m) depth of the basin (M. Bąbel, 1999*a*).

SUMMARY AND FINAL REMARKS

All the described facies record the sedimentary environments of the large 0–5 m deep evaporitic basin in which the facies variations depends mainly on salinity, depth and climate. Many facies have their equivalents in the recent shallow water evaporite environments: salinas and salt lakes. However, such facies as the giant intergrowths, wavy bedded sabre gypsum and microcrystalline gypsum (with halite traces) were deposited in peculiar environments (as described in this paper) thus far not observed in any modern setting. It is striking that the morphology of crystals from the giant intergrowths and grass-like facies was never observed in any other natural environments. Uncommon features of the studied evaporites might result from large sizes of the basin, however also from peculiar properties and composition of its brines (as suggested by some geochemical data: J. Parafiniuk, 1987; O. I. Petryczenko *et al.*, 1995; S. Hałas *et al.*, 1996; O. I. Petrichenko *et al.*, 1997; L. Rosell *et al.*, 1998). M. Bąbel (1994) supposed that peculiar organic substances in the brine (from decomposed terrestrial plants?) influened the morphology of gypsum. In sum, the described facies require further investigation for better understanding of their sedimentary environment.

Acknowledgements. This research was partly sponsored by the KBN grant 6 P04D 038 09. I wish to thank Grzegorz Czapowski, Andrzej Gąsiewicz and B. Charlotte Schreiber for their critical reviews, discussions and many constructive comments on earlier versions of the text. My special thanks are offered to Stefano Lugli, Juan Jose Pueyo Mur and B. Charlotte Schreiber who showed me salinas in Spain and on Sicily, which was very helpful in this facies study.

REFERENCES

ARAKEL A. V. (1980) — Genesis and diagenesis of Holocene evaporitic sediments in Hutt and Leeman Lagoons, western Australia. J. Sed. Petrol., 50 (4): 1305–1326.

AREF M. A. M. (1998) — Holocene stromatolites and microbial laminites associated with lenticular gypsum in a marine-dominated environment (Ras El Shetan area, Gulf of Aqaba, Egypt). Sedimentology, 45 (2): 245–262.

BATHURST R. G. C. (1971) — Carbonate sediments and their diagenesis. Develop. Sed., **12**. Elsevier. Amsterdam.

BĄBEL M. (1981) — Sedymentacja i wykształcenie facjalne gipsów nidziańskich. M.Sc. thesis. Arch. UW. Warszawa.

BĄBEL M. (1984) — Remarks on structure and development of *szklica* gypsum (in Polish with English summary). Prz. Geol., **32** (11): 577–582.

BĄBEL M. (1986) — Growth of crystals and sedimentary structures of the sabre-like gypsum (Miocene, southern Poland). Prz. Geol., **34** (4): 204–208.

BĄBEL M. (1987) — Giant gypsum intergrowths from the Middle Miocene evaporites of southern Poland. Acta Geol. Pol., **37** (1–2): 1–20.

BĄBEL M. (1990) — Crystallography and genesis of the giant intergrowths of gypsum from the Miocene evaporites of Poland. Arch. Miner., **44** (2): 103–135.

BĄBEL M. (1991) — Dissolution of halite within the Middle Miocene (Badenian) laminated gypsum of southern Poland. Acta Geol. Pol., **41** (3–4): 163–182.

BĄBEL M. (1994) — Geneza i morfologia kryształów gipsu w badeńskich ewaporatach Ponidzia. In: Neogeńskie ewaporaty środkowej Paratetydy — facje, surowce mineralne, ekologia: 3–4. Międzynarodowe Sympozjum, Lwów, 20–24 września 1994. Warszawa.

BĄBEL M. (1996) — Wykształcenie facjalne, stratygrafia oraz sedymentacja badeńskich gipsów Ponidzia. In: Analiza basenów sedymentacyjnych a nowoczesna sedymentologia (ed. P. H. Karnkowski): B1–B26. V Krajowe Spotkanie Sedymentologów. Warszawa.

BĄBEL M. (1998) — Paths of brine flow indicated by oriented gypsum crystals in the Badenian evaporitic basin of Carpathian Foredeep. In: 15th IAS Congress (Alicante, Spain), Abstracts: 160–161.

BĄBEL M. (1999*a*) — The roles of calcium deficiency and brine mixing in the origin of Badenian laminated gypsum deposits of Carpathian Foredeep. Intern. Symp. "Evaporates and carbonate-evaporate transitions". Abstracts. Lviv. Biul. Państw. Inst. Geol., **387**: 10–12.

BĄBEL M. (1999*b*) — History of sedimentation of the Nida Gypsum deposits (Middle Miocene, Carpathian Foredeep, southern Poland). Geol. Quart., **43** (4): 429–447.

BĄBEL M., BOGUCKIY A, VOLOSHIN P. (1998) — Isochronic correlation of the Miocene evaporites of Carpathian Foredeep over a distance of several hundred kilometres. In: 15th IAS Congress (Alicante, Spain), Abstracts: 161–162.

BERNER R. A. (1980) — Early diagenesis. A theoretical approach. Princeton University Press. Princeton, New Jersey.

BOBROWSKI W. (1963) — Gypsum in the eastern bank of the Nida river valley (in Polish with English summary). Biul. Inst. Geol. (without number): 1–29.

BURNE R. V., MOORE L. S. (1987) — Microbialites: organosedimentary deposits of benthic microbial communities. Palaios, **2** (3): 241–254.

BURNE R. V., MOORE L. S. (1993) — Microatoll microbialites of Lake Clifton, Western Australia: morphological analogues of *Cryptozoön proliferum* Hall, the first formally-named stromatolite. Facies, **29**: 149–168.

CODY R. D. (1991) — Organo-crystalline interactions in evaporite systems: the effects of crystallization inhibition. J. Sed. Petrol., **61** (5): 704–718.

CORNÉE A., DICKMAN M., BUSSON G. (1992) — Laminated cyanobacterial mats in sediments of solar works: some sedimentological implications. Sedimentology, **39** (4): 599–612.

DRONKERT H. (1977) — A preliminary note on a recent sabkha deposit in S. Spain. Inst. Invest. Geol. Diput. Prov., Univ. Barcelona, **32**: 153–166.

DRONKERT H. (1985) — Evaporite models and sedimentology of Messinian and Recent evaporites. GUA, Papers of Geology, Ser. 1, **24**.

DULAU N., TRAUTH N. (1982) — Etude des dépôts superficiels des marais salants de Salin de Giraud. Géol. Méditer., **9** (4): 501–520.

FERSMAN A. E. (1919) — On mineralogical and geological investigations of the Saki lake (in Russian). In: Academician A. E. Fersman, Collected works (ed. D. S. Belyankin), **1**: 809–822. Izd. Akad. Nauk USSR. Moscow, 1952.

FLIS J. (1954) — Gypsum karst of the Nida Trough (in Polish with English summary). Pr. Geogr. Inst. Geogr. PAN, **1**.

FRIEDMAN G. M., KRUMBEIN W. E. (eds.) (1985) — Hypersaline ecosystems; the Gavish Sabkha. Ecol. Stud., **53**. Springer-Verlag. Berlin.

GAWEŁ A. (1955) — Gypsum deposits in southern Poland (in Polish with English summary). Cement, **11/20** (6): 117–122.

GEISLER-CUSSEY D. (1986) — Approche sédimentologique et géochimique des mécanismes générateurs de formations évaporitiques actuelles et fossiles. Sci. Terre, Mém., **48**.

GEISLER-CUSSEY D. (1997) — Modern depositional facies developed in evaporative environments (marine, mixed, and nonmarine). In: Sedimentary deposition in rift and foreland basins in France and Spain (eds. G. Busson, B. C. Schreiber): 3–42. Columbia Univ. Press. New York.

GIANI D., SEELER J., GIANI L., KRUMBEIN W. E. (1989) — Microbial mats and physicochemistry in a saltern in the Bretagne (France) and a laboratory scale saltern model. FEMS Microbiol. Ecol., **62**: 151–162.

GOLDMAN M. I. (1952) — Deformation, metamorphism, and mineralization in gypsum-anhydrite cap rock, sulphur salt dome, Louisiana. Geol. Soc. Amer. Mem., **50**.

GOLONKA J. (1972) — Stromatolity z gipsów mioceńskich zatoki rzeszowskiej. Kwart. Geol., **16** (2): 494–495.

HAŁAS S., JASIONOWSKI M., PERYT T. M. (1996) — Isotopic anomaly in the Badenian gypsum of Nida River Valley (southern Poland) (in Polish only). Prz. Geol., **44** (10): 1054–1056.

HARDIE L. A., EUGSTER H. P. (1971) — The depositional environment of marine evaporites: a case for shallow, clastic accumulation. Sedimentology, **16** (3–4): 187–220.

HITE R. J., ANDERS D. E. (1991) — Petroleum and evaporites. In: Evaporites, petroleum and mineral resources (ed. J. L. Melvin). Develop. Sed., **50**: 349–411. Elsevier. Amsterdam.

KASPRZYK A. (1991) — Lithofacies analysis of the Badenian sulfate deposits south of the Holy Cross Mts. (in Polish with English summary). Prz. Geol., **39** (4): 213–223.

KASPRZYK A. (1993*a*) — Stromatolitic facies in the Badenian (middle Miocene) gypsum deposits of southern Poland. N. Jb. Geol. Paläont. Abh., **187** (3): 375–395.

KASPRZYK A. (1993*b*) — Lithofacies and sedimentation of the Badenian (Middle Miocene) gypsum in the northern part of the Carpathian Foredeep, southern Poland. Ann. Soc. Géol. Pol., **63** (1–3): 33–84.

KASPRZYK A. (1993*c*) — Gypsum facies in the Badenian (Middle Miocene) of southern Poland. Canad. J. Earth Sc., **30** (9): 1799–1814.

KASPRZYK A. (1995) — Gypsum-to-anhydrite transition in the Miocene of southern Poland. J. Sed. Res., **A65** (2): 348–357.

KASPRZYK A., ORTÍ F. (1998) — Paleogeographic and burial controls on anhydrite genesis: the Badenian basin in the Carpathian Foredeep (southern Poland, western Ukraine). Sedimentology, **45** (5): 889–907.

KREUTZ S. (1925) — W sprawie ochrony przyrody nieożywionej. Ochrona Przyrody, **5**: 58–68.

KRUMBEIN W. E., COHEN Y. (1977) — Primary production, mat formation and lithification: contribution of oxygenic and facultative anoxygenic cyanobacteria. In: Fossil algae (ed. E. Flügel): 37–56. Springer-Verlag. Berlin.

KUBICA B. (1992) — Lithofacial development of the Badenian chemical sediments in the northern part of the Carpathian Foredeep (in Polish with English summary). Pr. Państw. Inst. Geol., **133**.

KUSHNIR J. (1981) — Formation and early diagenesis of varved evaporite sediments in a coastal hypersaline pool. J. Sed. Petrol., **51** (4): 1193–1203.

KWIATKOWSKI S. (1970) — Origin of alabasters, intraformational breccias, folds and stromatolites in Miocene gypsum of Southern Poland. Bull. Acad. Pol. Sci., Sér. Sci. Géol. Géogr., **18** (1): 37–42.

KWIATKOWSKI S. (1972) — Sedimentation of gypsum in the Miocene of southern Poland (in Polish with English summary). Pr. Muz. Ziemi, **19**: 3–94.

KWIATKOWSKI S. (1974) — Miocene gypsum deposits in southern Poland (in Polish with English summary). Biul. Inst. Geol., **280**: 299–344.

LEPESHKOV I. N., BODALEVA N. V. (1952) — On crystallization sequence of salts during evaporation of Aral sea water (in Russian). Dokl. Akad. Nauk USSR, New Ser., **83** (4): 583–584.

LISZKOWSKI J. (1992) — Geneza środkowobadeńskiej (wielickiej) serii gipsowo-anhydrytowej zewnętrznego basenu zapadliska przedkarpackiego. In: Osady i procesy sedymentacji w środowiskach i systemach depozycyjnych w zapisie współczesnym i kopalnym (eds. J. Wojewoda, Z. Zwoliński). Przewodnik Seminarium Sedymentologicznego, Poznań: 125. Inst. Geol. UAM. Poznań.

LOGAN B. W. (1987) — The Macleod evaporite basin, western Australia. Mem. Amer. Ass. Petrol. Geol., **44**.

LOGAN B. W., REZAK R., GINSBURG R. N. (1964) — Classification and environmental significance of algal stromatolites. J. Geol., **72** (1): 68–83.

LOWENSTEIN T. (1982) — Primary features in a potash evaporite deposits, the Permian Salado Formation of the West Texas and New Mexico. In: Depositional and diagenetic spectra of evaporites (eds. C. G. Handford, R. G. Loucks, G. T. Davies). SEPM Core Workshop, **3**: 278–304. Calgary.

MUTTI E., RICCI LUCCHI F. (1975) — Turbidite facies and facies associations. In: Field trip guidebook A-11, Examples of turbidite facies and facies associations from selected formations of the Northern Apennines (eds. E. Mutti, G. C. Parea, F. Ricci Lucchi *et al.*): 21–36. 9th IAS Congress, Nice, France.

NIELUBOWICZ R. (1961) — Remarks concerning the stratigraphy of several Miocene gypsum layers in the west zones of Subcarpathian Depression (in Polish only). Cement, **16/26** (3): 68–77.

NIEMCZYK J. (1985) — Laminated gypsum from allochthonous Miocene of the Rzeszów region (in Polish with English summary). Geol. Kwart. AGH, **11** (2): 109–119.

NIEMCZYK J. (1988*a*) — On some aspects of gypsum lamination at Krzyżanowice near Pińczów (in Polish with English summary). Geol. Kwart. AGH, **14** (2): 75–80.

NIEMCZYK J. (1988*b*) — Gypsum-arenites of the Miocene evaporitic series in the Wiślica Region (in Polish with English summary). Geol. Kwart. AGH, **14** (3): 51–56.

NIEMCZYK J. (1988*c*) — Lithostratigraphy of Miocene gypsum deposits between Busko and Wiślica (in Polish with English summary). Geol. Kwart. AGH, **14** (3): 105–114.

NIEMCZYK J. (1995) — Geological section at Krzyżanowice near Pińczów as a base for lithostratigraphy of the Gypsum Formation of the Nida region (Southern Poland) (in Polish with English summary). Geol. Kwart. AGH, **21** (3): 183–196.

ORTÍ CABO F., PUEYO MUR J. J., GEISLER-CUSSEY D., DULAU N. (1984) — Evaporitic sedimentation in the coastal salinas of Santa Pola (Alicante, Spain). Rev. Inst. Invest. Geol., **38/39**: 169–220.

PARAFINIUK J. (1987) — Strontium and barium in the sulphur-bearing Miocene deposits of the northern part of the Carpathian Foredeep (SE Poland) (in Polish with English summary). Arch. Miner., **43** (1): 87–143.

PERYT T. M. (1996) — Sedimentology of Badenian (middle Miocene) gypsum in eastern Galicia, Podolia and Bukovina (West Ukraine). Sedimentology, **43** (3): 571–588.

PERYT T. M., JASIONOWSKI M. (1994) — In situ formed and redeposited gypsum breccias in the Middle Miocene Badenian of southern Poland. Sed. Geol., **94** (1–2): 153–163.

PERYT T. M., KASPRZYK A. (1992*a*) — Earthquake-induced resedimentation in the Badenian (middle Miocene) gypsum of southern Poland. Sedimentology, **39** (2): 235–249.

PERYT T. M., KASPRZYK A. (1992*b*) — Carbonate-evaporite sedimentary transitions in the Badenian (middle Miocene) basin of southern Poland. Sed. Geol., **76** (3–4): 257–271.

PERYT T. M., POBEREZHSKY A., YASINOVSKY M. (1995) — Facies of Badenian gypsum of the Dnister River region (in Ukrainian with English summary). Geol. Geokhim. Goriuchykh Kopalyn (Lviv), **1–2**: 16–27.

PERYT T. M., POBEREŻSKI A., JASIONOWSKI M., PETRYCZENKO O. I., PERYT D., RYKA W. (1994) — Badenian gypsum facies in the Nida and Dnister river-basins (southern Poland and SW Ukraine) (in Polish only). Prz. Geol., **42** (9): 771–776.

PETRICHENKO O. I., PERYT T. M., POBEREGSKY A. (1997) — Peculiarities of gypsum sedimentation in the Middle Miocene Badenian evaporite basin of Carpathian Foredeep. Slovak Geol. Mag., **3** (2): 91–104.

PETRYCZENKO O. I., PERYT T. M., POBEREŻSKI A., KASPRZYK A. (1995) — Inclusions of microorganisms in the Middle Miocene Badenian gypsum crystals of the Carpathian Foredeep (in Polish with English summary). Prz. Geol., **43** (10): 859–862.

REINECK H. E., GERDES G., CLAES M., DUNAJTSCHIK K., RIEGE H., KRUMBEIN W. E. (1990) — Microbial modification of sedimentary surface structures. In: Sediments and environmental geochemistry (eds. D. Heling, P. Rothe, U. Förstner, P. Stoffers): 254–276. Springer-Verlag. Berlin.

RICHTER-BERNBURG G. (1973) — Facies and paleogeography of the Messinian evaporites on Sicily. In: Messinian events in the Mediterranean (ed. C. W. Drooger): 124–141. North Holland Publ. Comp. Amsterdam.

ROMAN A. (1999) — Brine paleocurrents reconstructed from orientation of the gypsum crystals on the Miechów Upland, Southern Poland. Intern. Symp. "Evaporates and carbonate-evaporate transitions". Abstracts. Lviv. Biul. Państw. Inst. Geol., **387**: 60–62.

ROSELL L., ORTÍ F., KASPRZYK A., PLAYÁ E., PERYT T. M. (1998) — Strontium geochemistry of Miocene primary gypsum: Messinian of SE Spain and Sicily and Badenian of Poland. J. Sed. Res., **68** (1): 63–79.

ROUCHY J. M. (1982) — La genèse des évaporites messiniennes de Méditerrannée. Mém. Mus. Nat. Hist. Nat., Sér. C, Sc. Terre, **50**.

ROUCHY J. M., MONTY C. L. V. (1981) — Stromatolites and cryptalgal laminites associated with Messinian gypsum of Cyprus. In: Phanerozoic stromatolites (ed. C. L. V. Monty): 155–180. Springer-Verlag. Berlin.

SANDER B. (1970) — An introduction to the study of fabrics of geological bodies (transl. from German publications printed in 1948, 1950). Pergamon Press. Oxford.

SCHREIBER B. C. (1978) — Environments of subaqueous gypsum deposition. In: Marine evaporites (eds. E. Dean, B. C. Schreiber). SEPM Short Course, **4**: 43–73. Oklahoma City.

SCHREIBER B. C., CATALANO R., SCHREIBER E. (1977) — An evaporitic lithofacies continuum: latest Miocene (Messinian) deposits of Salemi basin (Sicily) and a modern analog. In: Reefs and evaporites — concepts and models (ed. J. H. Fisher). AAPG Stud. Geol., **5**: 169–180.

SCHREIBER B. C., FRIEDMAN G. M., DECIMA A., SCHREIBER E. (1976) — Depositional environments of Upper Miocene (Messinian) evaporite deposits of the Sicilian Basin. Sedimentology, **23** (6): 729–760.

SCHREIBER B. C., ROTH M. S., HELMAN M. L. (1982) — Recognition of primary facies characteristics of evaporites and differentiation of these forms from diagenetic overprints. In: Depositional and diagenetic spectra of evaporites (eds. C. G. Handford, R. G. Loucks, G. T. Davies). SEPM Core Workshop, **3**: 1–32. Calgary.

SŁOMKA T. (1979) — Manifestations of cyclicity in sedimentation of Miocene laminated gypsum (in Polish with English summary). Geol. Kwart. AGH, **5** (4): 59–65.

VAI G. B., RICCI LUCCHI F. (1977) — Algal crusts, autochthonous and clastic gypsum in a cannibalistic evaporite basin: a case story from the Messinian of Northern Apennines. Sedimentology, **24** (2): 211–244.

WALA A. (1963) — Korelacja litostratygraficzna profili serii gipsowej obszaru nadnidziańskiego. Spraw. z Pos. Komis. PAN, Kraków, lipiec–grudzień 1962: 530–532.

WALA A. (1980) — Litostratygrafia gipsów nidziańskich (fm). In: Gipsy niecki nidziańskiej i ich znaczenie surowcowe: 5–10. Symp nauk. Kraków.

WALTER M. R. (1976) — Introduction. In: Stromatolites (ed. M. R. Walter), Develop. Sed., **20**: 1–3. Elsevier. Amsterdam.

WARREN J. K. (1982) — The hydrological setting, occurrence and significance of gypsum in late Quaternary salt lakes in South Australia. Sedimentology, **29** (5): 609–637.

FACJE I ŚRODOWISKA DEPOZYCJI BADEŃSKICH GIPSÓW PONIDZIA

Streszczenie

W badeńskich gipsach Ponidzia wyróżniono 6 facji siarczanowych: gipsy szklicowe, rumosze kryształów gipsu, gipsy trawiaste, szablaste, mikrokrystaliczne, porfiroblastyczne i jedną fację węglanową. W obrębie 5 pierwszych facji wyróżniono 12 subfacji i scharakteryzowano środowiska ich sedymentacji, które w większości są typowe dla płytkiego, okresowo wynurzanego zbiornika ewaporacyjnego.

Facje zdefiniowano jako produkty kilku podstawowych mechanizmów depozycyjnych (por. E. Mutti, F. Ricci Lucchi, 1975), m.in. takich jak: (I) syntaksjalny wzrost dużych kryształów gipsu wprost na dnie basenu (gipsy szklicowe, trawiaste i szablaste), (II) mikrobialną (*sensu* R. V. Burne, L. S. Moore, 1987) depozycję drobnokrystalicznego gipsu, głównie poprzez gipsyfikację mat organicznych (gipsy trawiaste), (III) depozycję mechaniczną (gipsy mikrokrystaliczne), obejmującą opadanie i osiadanie drobnych kryształów gipsu wytrącanych w toni wodnej, oraz redepozycję osadu gipsowego. Zróżnicowanie facjalne gipsów Ponidzia wynika przede wszystkim z wahań zasolenia i głębokości basenu oraz wilgotności klimatu.

EXPLANATIONS OF PLATES

PLATE I

Giant gypsum intergrowths showing skeletal palisade structure and dissolution surfaces (arrowed). Leszcze quarry

PLATE II

Fig. 1. Lower part of the Nida Gypsum deposits at Borków quarry. Convexietes below the giant intergrowths result from sinking of the growing crystals into muddy substrate

Fig. 2. Single intergrowths and aggregates of gypsum crystals growing separately on muddy substrate. Samples collected along the base surface of giant intergrowths seen in Fig. 1

PLATE III

Fig. 1. Non-palisade subfacies of the giant gypsum intergrowths. Chwałowice

Fig. 2. Debris of gypsum crystals covering the giant intergrowths. Sielec Rządowy; detail from pl. I, fig. 1 in M. Bąbel (1999*b*)

PLATE IV

Fig. 1. Intraclasts of early cemented gypsum (mainly gypsified organic mats, some of them coverd with bottom-grown crystals, dark), redeposited by sheet flood. Subfacies of grass-like gypsum with clay intercalations. Leszcze quarry, layer **d**

Fig. 2. Channel (C), infilled with clastic gypsum, within grass-like subfacies with clay intercalations overlying giant intergrowths. Gorysławice, near gasoline station

PLATE V

Fig. 1. Grass-like gypsum, subfacies with clay intercalations. Layer containing alabaster domes covered with gypsum crystals is arrowed. Skorocice nature reserve, layer **e**

Fig. 2. Microbial alabaster dome covered with crusts of bottom-grown gypsum crystals developed on gypsified organic mats. Abandoned quarry at Gacki. Photo by S. Ulatowski

PLATE VI

Fig. 1. Gypsified organic mats. Borków quarry, layer **c**. Photo by S. Ulatowski

Fig. 2. Grass-like gypsum crystals intercalated with alabaster beds. Chotel Czerwony–Zagórze, layers **b**, **c** shown in A. Kasprzyk (1993*a*, pl. IV) and M. Bąbel (1999*b*, pl. II, fig. 2)

PLATE VII

Fig. 1. Rows of gypsum crystals with large fenestral pores (pen for scale). Borków quarry, layer **b**

Fig. 2. Stromatolitic gypsum domes. Borków quarry, layer **e**

PLATE VIII

Fig. 1. Aggregates of sabre gypsum crystals scattered within microbial gypsum. Note horizontal disappearing of lamination interpreted as a result of selective early cementation. Leszcze quarry, layer **i**

Fig. 2. Rows of bottom-grown sabre gypsum crystals showing synsedimentary dissolution surfaces (arrowed). Skorocice nature reserve, layer **g**

PLATE IX

Fig. 1. Laminated gypsum showing wash-out structure (arrowed). Leszcze quarry

Fig. 2. Laminated gypsum with intercalations of halite-solution residual "alabaster" (arrowed). Leszcze quarry. Photo by S. Ulatowski

PLATE X

Fig. 1. Halite-solution residual "alabasters" and collapse breccias within laminated gypsum. Leszcze quarry

Fig. 2. Residual solution-subsidence gypsum deposits with traces after halite crystals (marked **h**). Leszcze quarry, layer **k**

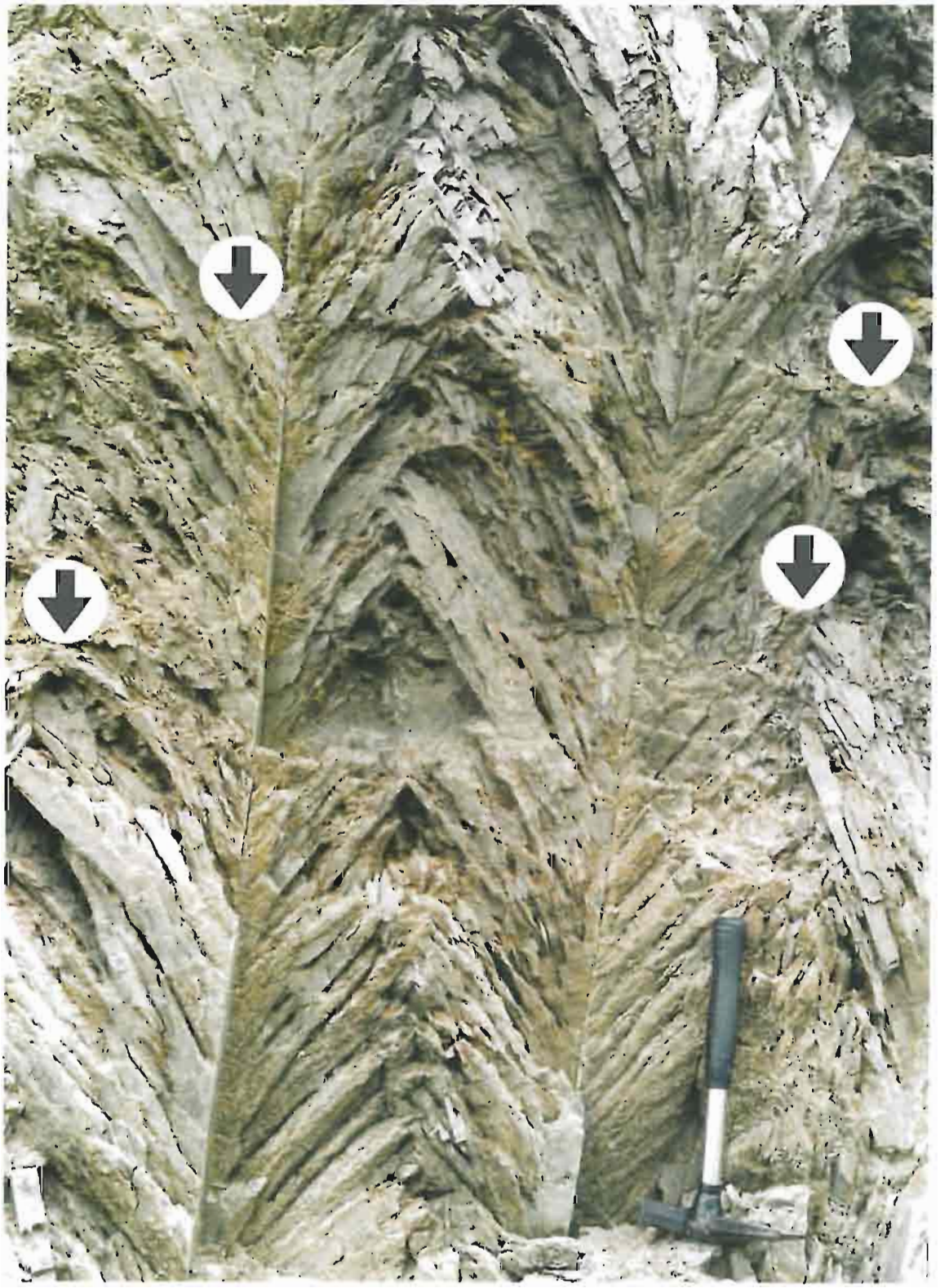

Maciej BĄBEL — Facies and depositional environments of the Nida Gypsum deposits (Middle Miocene, Carpathian Foredeep, southern Poland)

Geol. Quart., 1999, 43 (4)

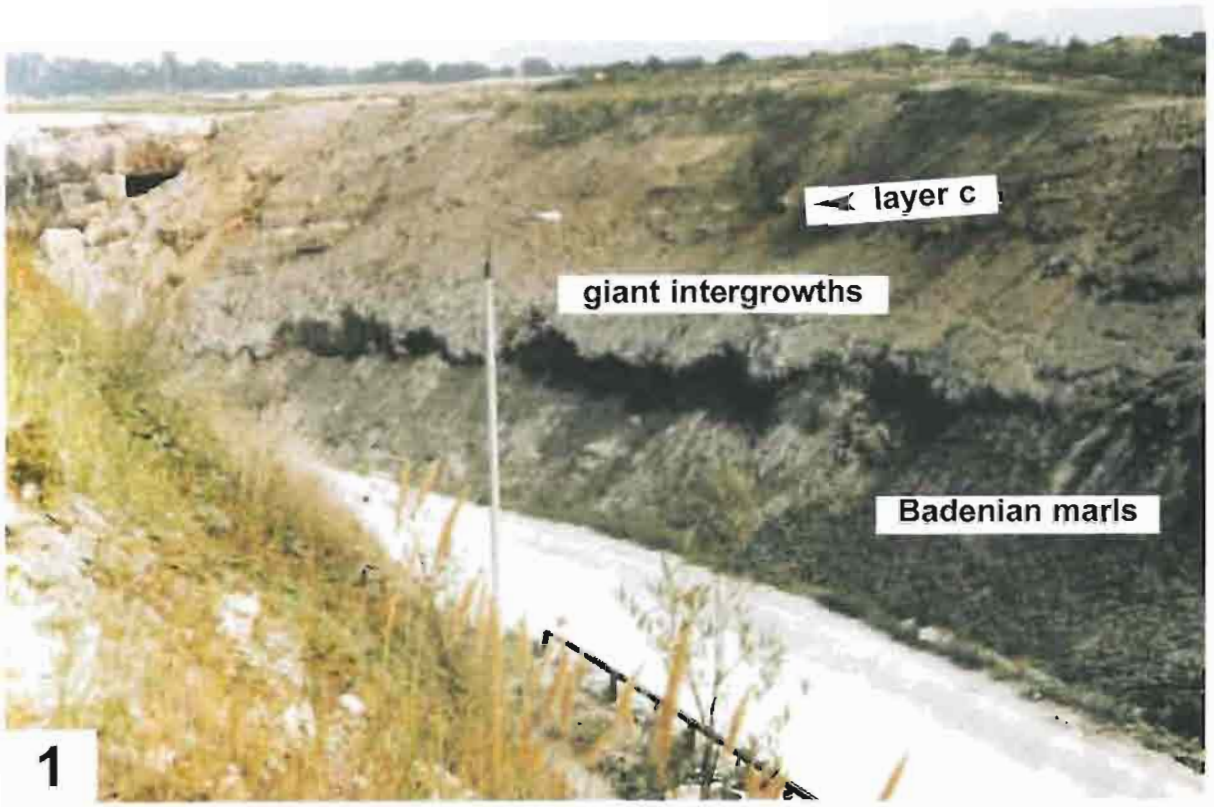

Maciej BĄBEL — Facies and depositional environments of the Nida Gypsum deposits (Middle Miocene, Carpathian Foredeep, southern Poland)

Maciej BĄBEL — Facies and depositional environments of the Nida Gypsum deposits (Middle Miocene, Carpathian Foredeep, southern Poland)

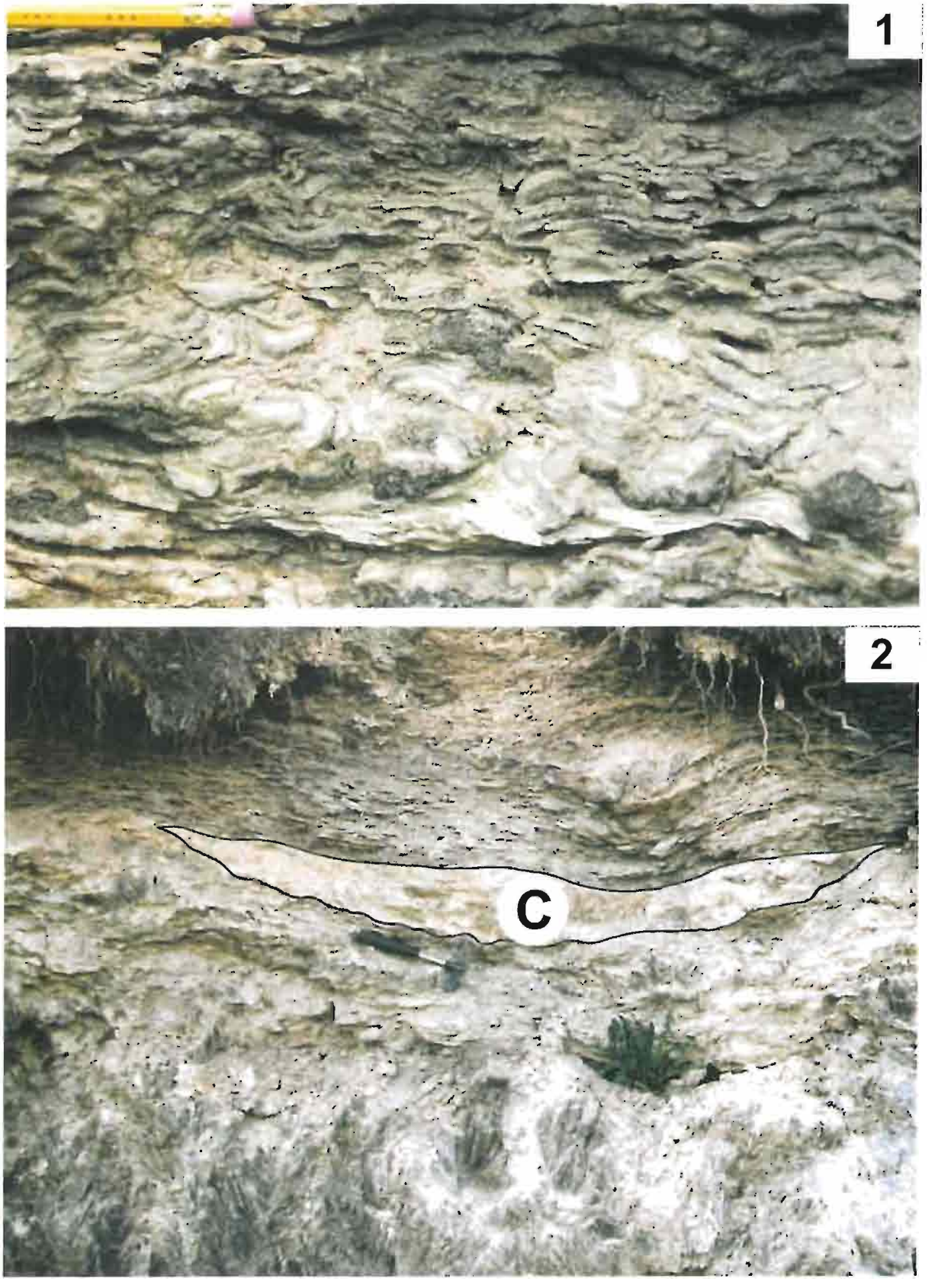

Maciej BĄBEL — Facies and depositional environments of the Nida Gypsum deposits (Middle Miocene, Carpathian Foredeep, southern Poland)

Maciej BĄBEL — Facies and depositional environments of the Nida Gypsum deposits (Middle Miocene, Carpathian Foredeep, southern Poland)

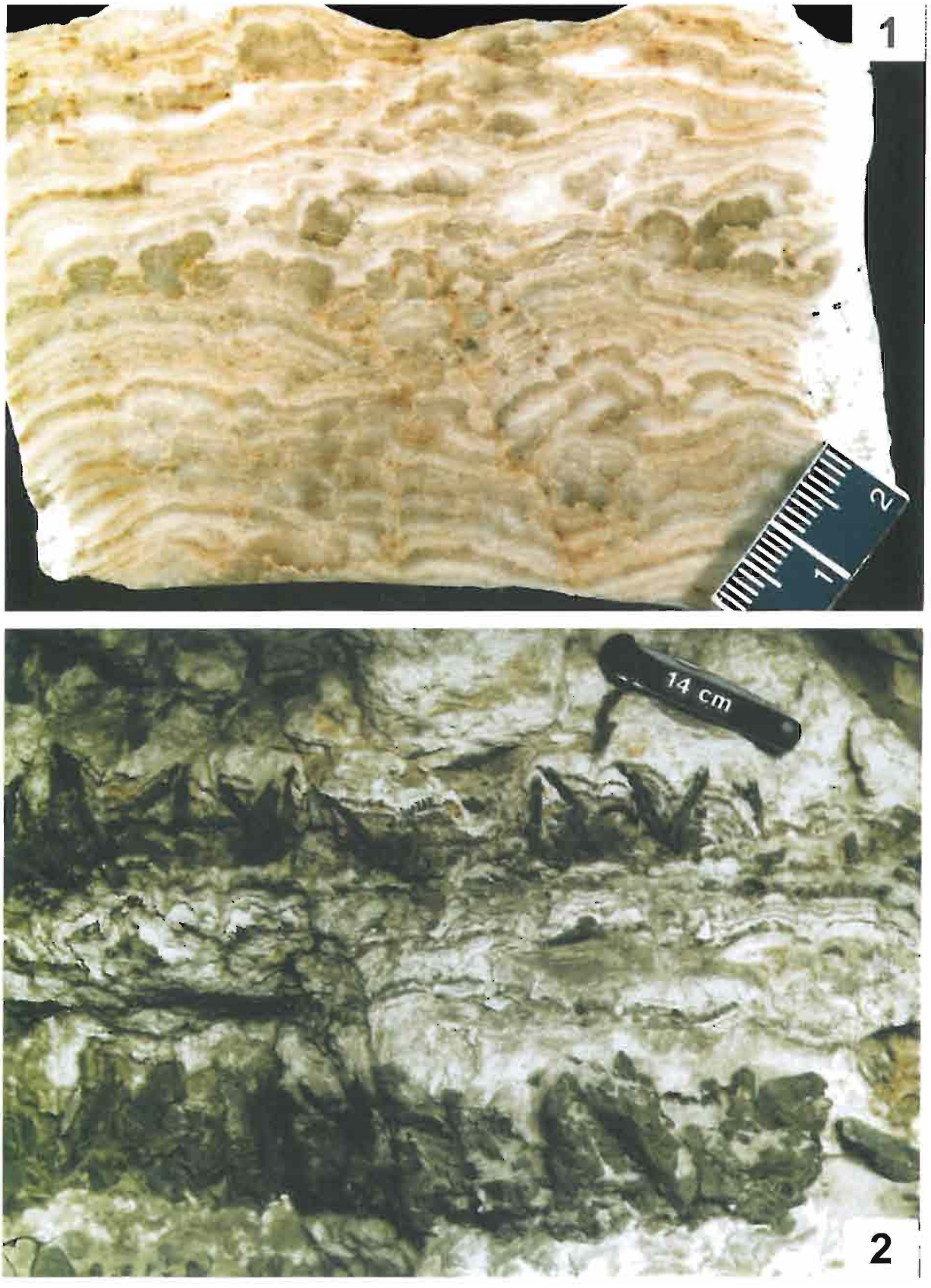

Maciej BĄBEL — Facies and depositional environments of the Nida Gypsum deposits (Middle Miocene, Carpathian Foredeep, southern Poland)

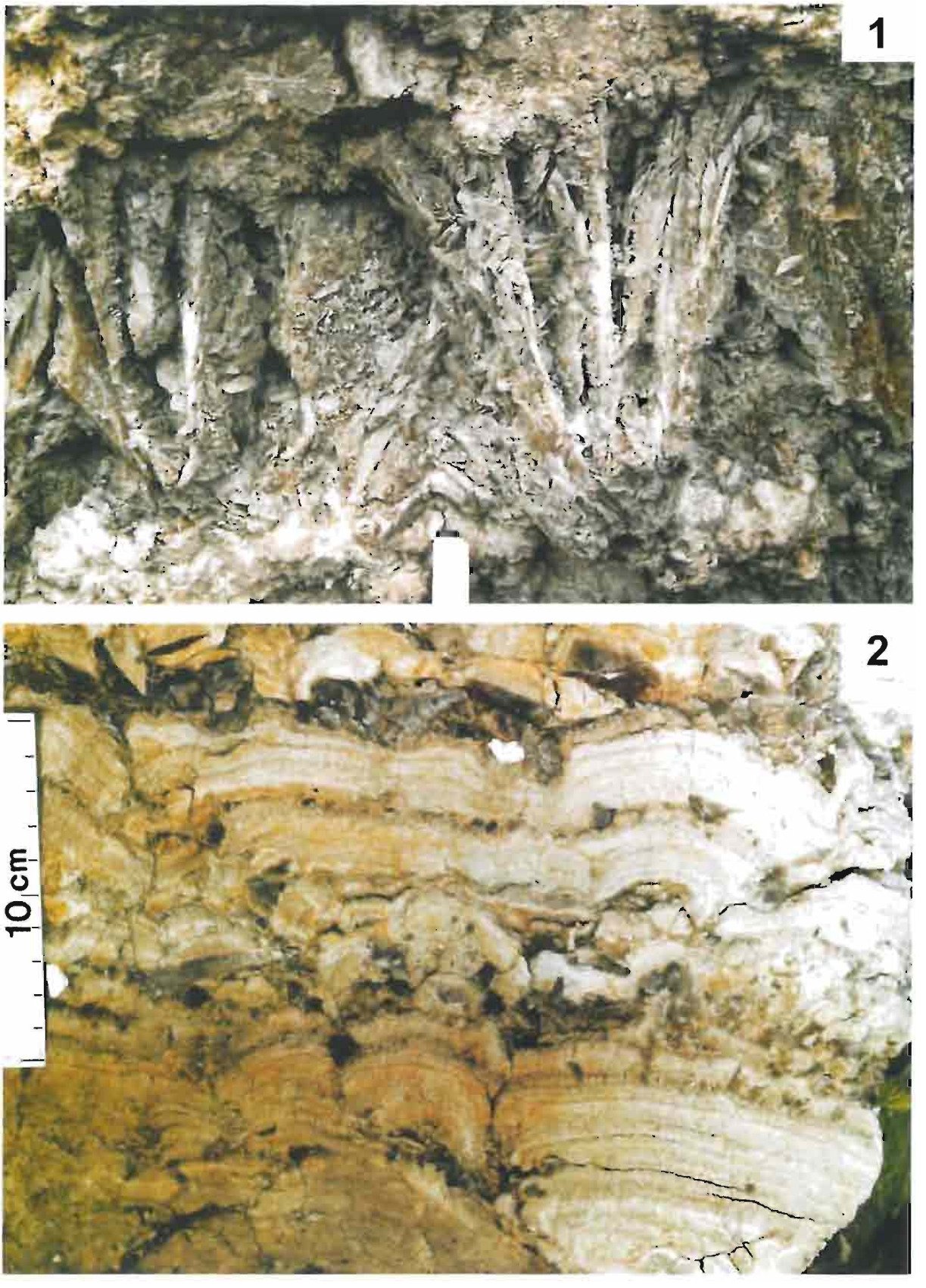

Maciej BĄBEL — Facies and depositional environments of the Nida Gypsum deposits (Middle Miocene, Carpathian Foredeep, southern Poland)

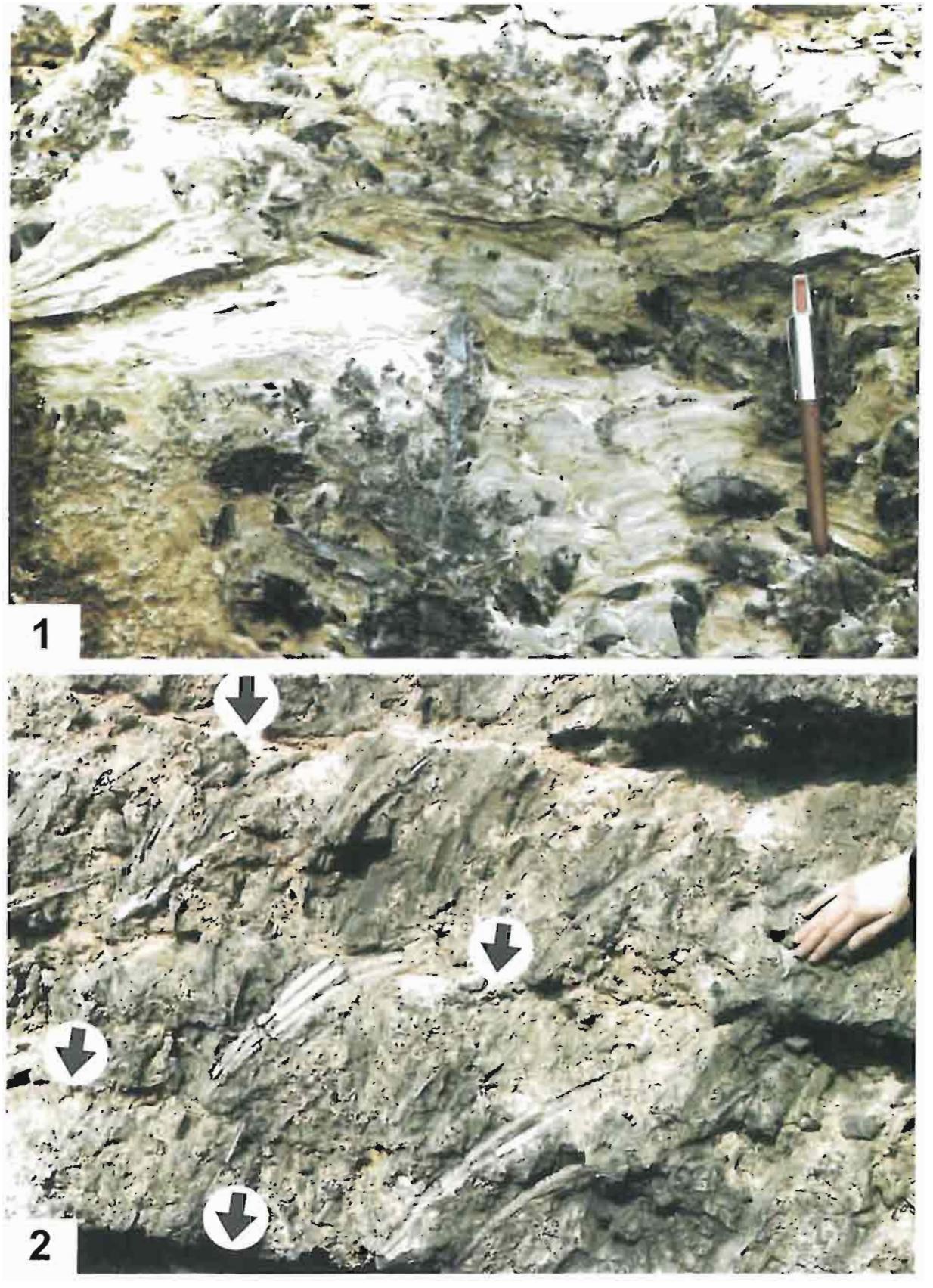

Maciej BĄBEL — Facies and depositional environments of the Nida Gypsum deposits (Middle Miocene, Carpathian Foredeep, southern Poland)

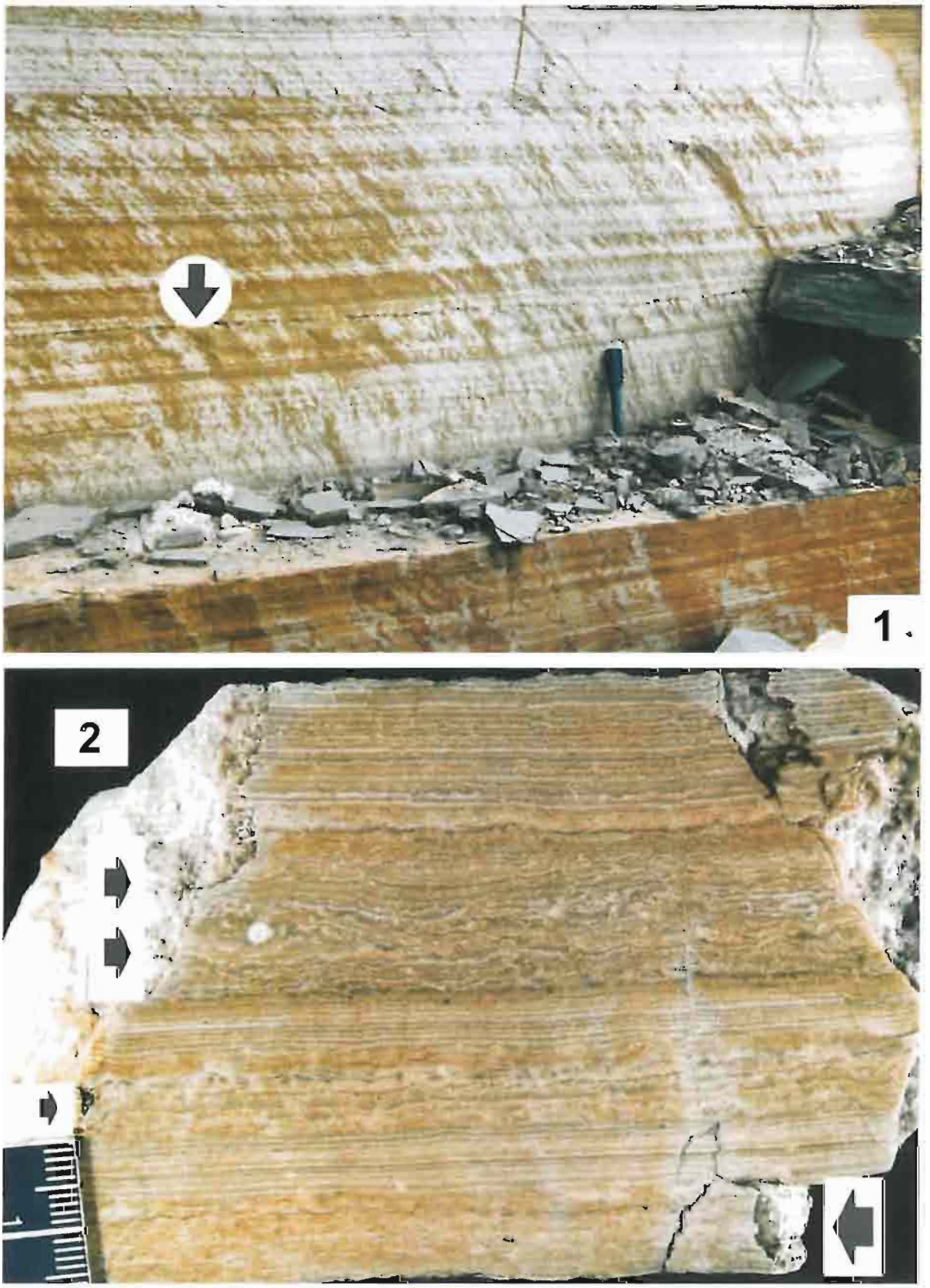

Maciej BĄBEL — Facies and depositional environments of the Nida Gypsum deposits (Middle Miocene, Carpathian Foredeep, southern Poland)

Geol. Quart., 1999, 43 (4)

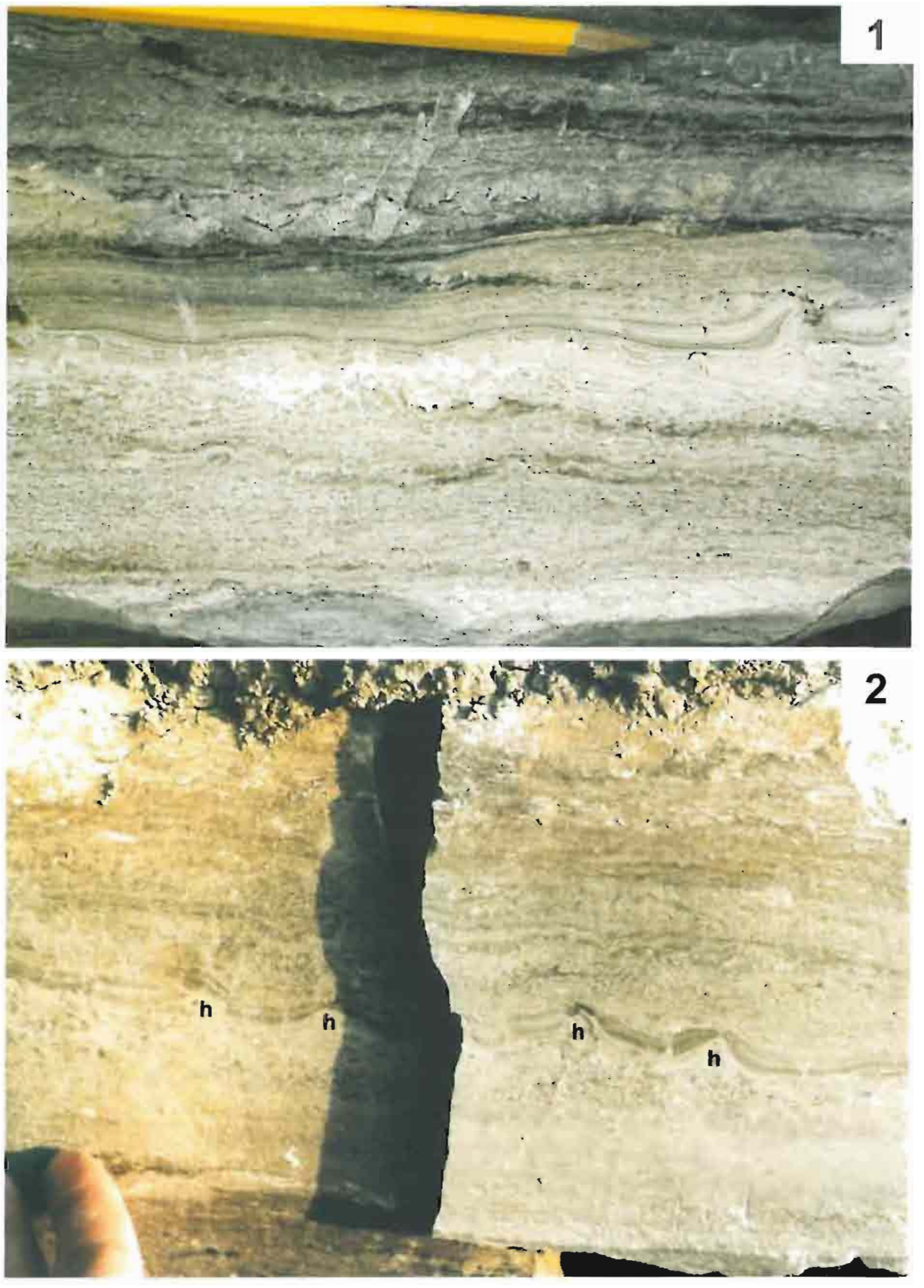

Maciej BĄBEL — Facies and depositional environments of the Nida Gypsum deposits (Middle Miocene, Carpathian Foredeep, southern Poland)